Biogeosciences Discuss., 12, 18253–18313, 2015
www.biogeosciences-discuss.net/12/18253/2015/
doi:10.5194/bgd-12-18253-2015

Biogeosciences Discussions
Open Access
EGU

Bathypelagic particle flux signatures from a suboxic eddy in the oligotrophic tropical North Atlantic: production, sedimentation and preservation

G. Fischer[1,2], J. Karstensen[3], O. Romero[2], K.-H. Baumann[1,2], B. Donner[2], J. Hefter[2,4], G. Mollenhauer[2,4], M. Iversen[2,4], B. Fiedler[3], I. Monteiro[5], and A. Körtzinger[3]

[1]FB Geosciences, University of Bremen, Klagenfurter Str., 28359 Bremen, Germany
[2]Marum Centre for Marine Environmental Sciences, Leobener Str., University of Bremen, 28334 Bremen, Germany
[3]GEOMAR Helmholtz Center for Ocean Research Kiel, Düsternbrooker Weg 20, 24105 Kiel, Germany
[4]Alfred Wegener Institute, Helmholtz Center for Polar and Marine Sciences, 27570 Bremerhaven, Germany
[5]Instituto Nacional de Desenvolvimento das Pescas (INDP), Cova da Inglesa, CP132, Mindelo, São Vicente, Cabo Verde, Africa

Received: 30 October 2015 – Accepted: 3 November 2015 – Published: 13 November 2015

Correspondence to: G. Fischer (gerhard.fischer@uni-bremen.de)

Published by Copernicus Publications on behalf of the European Geosciences Union.

BGD
12, 18253–18313, 2015

Abstract

Particle fluxes at the Cape Verde Ocean Observatory (CVOO) in the eastern tropical North Atlantic for the period December 2009 until May 2011 are discussed based on bathypelagic sediment trap time series data collected at 1290 and 3439 m water depth. The typically oligotrophic particle flux pattern with weak seasonality is modified by the appearance of a highly productive and low oxygen anticyclonic modewater eddy (ACME) in winter 2010. The eddy passage was accompanied by unusually high mass fluxes, lasting from December 2009 to May 2010. Distinct biogenic silica (BSi) and organic carbon flux peaks were observed in February–March 2010 when the eddy approached CVOO. The flux of the lithogenic component, mostly mineral dust, was well correlated to that of organic carbon in particular in the deep trap samples, suggesting a close coupling. The lithogenic ballasting obviously resulted in high particle settling rates and, thus, a fast transfer of epi-/mesopelagic signatures to the bathypelagic traps. Molar C : N ratios of organic matter during the ACME passage were around 18 and 25 for the upper and lower trap samples, respectively. This suggests that some production under nutrient (nitrate) limitation in the upper few tens of meters above the zone of suboxia might have occurred in the beginning of 2010. The δ^{15}N record showed a decrease from January to March 2010 while the organic carbon and N fluxes increased. The causes of enhanced sedimentation from the eddy in February/March 2010 remain elusive but nutrient depletion and/or a high availability of dust as ballast mineral for organic-rich aggregates might have contributed to the elevated fluxes during the eddy passage. Remineralization of sinking organic-rich particles could have contributed to the formation of a suboxic zone at shallow depth. Although the eddy has been formed in the African coastal area in summer 2009, no indication of coastal flux signatures were found in the sediment traps, suggesting an alteration of the eddy since its formation. This confirms the assumption that suboxia developed within the eddy en-route. Screening of the biomarker fractions for the occurrence of ladderane fatty acids that could indicate the presence of anammox (anaeobic ammonia oxidation) bacteria, and isore-

BGD
12, 18253–18313, 2015

nieratene derivatives, indicative for the presence of green sulfur bacteria and, thus for photic zone suboxia/anoxia was negative. This could indicate that suboxic conditions in the eddy had recently developed and the respective bacterial stocks had not yet reached detection thresholds. Another explanation is that the fast sinking organic-rich particles produced in the surface layer did not interact with bacteria from the suboxic zone below. Carbonate fluxes dropped considerably in February 2010, mainly due to reduced contribution of shallow dwelling planktonic foraminifera and pteropods. The deep-dwelling foraminifera *Globorotalia menardii*, however, showed a major flux peak in February 2010, most probably due to the suboxia/hypoxia. The low oxygen conditions forced at least some zooplankton to stop diel vertical migration. Reduced "flux feeding" by zooplankton in the epipelagic could have contributed to the enhanced fluxes of organic materials to the bathypelagic traps during the eddy passage.

1 Introduction

Time-series particle flux studies have been performed in many ocean areas including typical oligotrophic settings in the Atlantic and the Pacific (BATS, HOT, ESTOC; e.g. Karl et al., 1996, 2003; Neuer et al., 2002, 2007; Lampitt and Antia, 1997; Honjo et al., 2008) and in Eastern Boundary Upwelling Ecosystems (EBUE) (e.g. Fischer et al., 2010; Romero et al., 2002). In general, seasonality is low in areas with low primary production while it increases towards coastal and open ocean high production (equatorial, polar) settings (Berger and Wefer, 1990; Romero and Armand, 2010). Mass fluxes at the French oligotrophic EUMELI site (ca. 21° N, 31° W) located NW of the Cape Verde Ocean Observatory (CVOO) study site were rather low (mostly below 60 $mg\,m^{-2}\,d^{-1}$) with a low to moderate seasonality (Bory et al., 2001).

In near coastal areas, particle fluxes can vary dramatically due to productivity events triggered by upwelling and submesoscale frontal processes such as filaments (Fischer et al., 2009). In the open ocean outside of frontal regions, productivity events are mostly related to the occurrence of mesoscale eddies (Benitez-Nelson and McGul-

BGD
12, 18253–18313, 2015

licuddy, 2008). However, a flux signature from an eddy in the deep ocean has not yet been described using sediment traps or radionuclides (e.g. Buesseler et al., 2007). This might be due to undersampling and the episodic nature of pulses of organic matter from mesoscale eddies. In the quiescent shadow zone region of the eastern tropical North Atlantic (Luyten et al., 1983), mesoscale eddies originate mostly from energetic flow in the coastal/open ocean transition zone of the West African coast. After formation, the eddies propagate westward into the open North Atlantic, typically at certain latitudes which may be considered as eddy corridors (Schütte et al., 2015a). The CVOO mooring site (Fig. 1), about 100 km north of the Cape Verde Island São Vicente, is located in such an eddy corridor. Considering rotation as well as the vertical structure of eddies, three types may be distinguished (Schütte et al., 2015b): cyclonic, anticyclonic, and anticyclonic modewater eddies (ACME). In particular, ACMEs have been reported in the past to support high productivity and chlorophyll standing stock (McGuillicuddy et al., 2007), primarily related to a very shallow mixed layer base in the eddy and the efficiency in vertical transport of nutrients into the euphotic zone. A comprehensive overview to mesoscale eddies including ACMEs and their physical and biogeochemical linkages is given by Benitez-Nelson and McGullicuddy (2008). Multi-year oxygen time series data from CVOO show frequent sudden drops in oxygen concentration associated with the passage of ACMEs (Karstensen et al., 2015a). One particularly strong event lasted the entire February 2010 with lowest oxygen concentrations of only 1–2 µmol kg^{-1} at about 40 m depth (Karstensen et al., 2015a). Using satellite data, the propagation path of this particular ACME has been reconstructed and found to have formed in summer 2009, at about 18° N at the West African coast (Fig. 1).

Here we describe particle flux signatures of the passage of this ACME crossing CVOO in February 2010. We will make use of monthly catches (29 day intervals) from bathypelagic sediment traps installed at 1290 and 3439 m for the period from December 2009 to March 2011 (Table 1). The total length of the sediment trap data time series of about 16 months allows us to compare the winter 2009–2010 with an ACME passage to the winter 2010–2011 without an ACME passage in the vicinity of the moor-

BGD
12, 18253–18313, 2015

ing site. We present and discuss fluxes of main phytoplankters (e.g. diatoms, coccolithophores) and secondary producers of carbonate (e.g planktonic foraminifera). Stable nitrogen isotope ratios and biomarker studies complement this multi-proxy approach of an ACME passage. We will discuss how and why the flux signatures from the eddy in the surface-subsurface ocean were transferred to the meso-bathypelagic ocean. We further consider effects of particle production in the surface waters versus preservation of organic materials settling through the suboxic/hypoxic zone of the ACME, the latter zone being characterized by a reduced diel vertical migration of zooplankton. We also address the question of when the suboxia/hypoxia developed in the history of the eddy. Our work is a contribution to a dedicated experiment, conducted in spring 2014, where ship-based and autonomous observations were performed to investigate ecology, biogeochemistry, and physical processes in low oxygen eddies in greater detail (Löscher et al., 2015b; Hauss et al., 2015; Schütte et al., 2015b; Fiedler et al., 2015; Karstensen et al., 2015b).

2 Oceanographic, biological and atmospheric setting at CVOO

The Cape Verde Ocean Observatory (CVOO) is located in the oligotrophic North Atlantic, far west of the coastal upwelling of the Canary Current System (Barton et al., 1998), one of the major Eastern Boundary Upwelling Ecosystems (EBUE; Freon et al., 2009). A distinct hydrographic boundary exists northwest of CVOO, the Cape Verde Frontal Zone (CVFZ, Zenk et al., 1991), separating the eastern boundary shadow zone with sluggish flow, low oxygen and high nutrient waters from the well-ventilated, high oxygen and nutrient-poorer waters to the west. The different coastal upwelling systems within the Canary Current with respect to production/phytoplankton standing stock and seasonality have been described recently by Cropper et al. (2014).

Monthly maps of surface chlorophyll concentrations derived from ocean color data in the CVOO area show mostly concentrations below 0.25 $mg\,m^{-3}$ (Fig. 1). A slight increase on surface chlorophyll is seen during boreal winter months where concen-

BGD
12, 18253–18313, 2015

trations up to 0.5 mg m^{-3} are found. The high cloud coverage partly prohibits detailed analysis of the surface chlorophyll concentrations. From the few high resolution daily maps available during the CVOO-3 period (Fig. 1), locally enhanced surface chlorophyll can be identified that coincide with westward propagation of mesoscale eddies, as reported before (e.g. Benitez-Nelson and McGullicuddy, 2008). The eddies form in spring and summer at the African coast, in the area between Cape Blanc and Cape Vert, Senegal (around 15 and 20° N), and propagate westward with about 5 km day^{-1} (Schütte et al., 2015a). Some of the eddies, in particular the ACMEs, develop low dissolved oxygen (DO) concentrations at very shallow depth (Karstensen et al., 2015a). It has been proposed that the low DO concentrations are created within the eddies through intense respiration, associated with high particle fluxes, and sluggish ventilation of the eddy core. During CVOO-3, one particular high productive/low oxygen ACME passed the CVOO site over a period of about one month, in February 2010 (Figs. 1, 3).

The ocean area off West Africa receives the highest supply of dust of the world (Schütz et al., 1981; Goudie and Middleton, 2001; Kaufman et al., 2005; Schepanski et al., 2009). Dust is not only relevant for the climate system (e.g. Ansmann et al. 2011; Moulin et al., 1997) and the addition of nitrate, phosphate and iron to the surface ocean (e.g. Jickells et al., 1998), but also for the ballasting of organic-rich particles (Iversen and Ploug, 2010; Ploug et al., 2008; Fischer and Karakas, 2009) formed in the surface ocean ("ballast theory", Armstrong et al., 2002; Ittekkot, 1993). Mineral dust has been shown to contribute about 1/3 and 1/2 of the total deep ocean mass flux off Cape Blanc and south of the Cape Verdes (CV-1-2 trap, ca. 11°30′ N / 21° W; Ratmeyer et al., 1999), respectively. Typically, mineral dust correlates with the satellite-based annual aerosol optical index (Fischer et al., 2010) and high dust fluxes have been found at the oligotrophic EUMELI site at around 21° N/31° W far north of CVOO (Bory et al., 2001). We obtained a mean annual dust flux of 14 g m^{-2} yr^{-1} for the eastern North Atlantic off West Africa (Fischer et al., 2009a). This is in accordance with other studies including modelling approaches (e.g. Kaufman et al., 2005; Jickells et al., 2005). Grain size studies from Ratmeyer et al. (1999) showed dust particles in the

BGD
12, 18253–18313, 2015

range of 10–15 µm at the CV-1-2 sediment trap mooring site at 1000 m water depth south of the Cape Verdes, with slightly smaller sizes in winter–spring. On the Cape Verde Islands in Praia, however, much smaller grain sizes, often below < 1 µm, were observed (from alumosilicates), pointing to gravitational settling processes during dust transport from Africa to the open ocean (Ansmann et al., 2011). Seasonality, mass concentrations and long-term chemical characterization of Saharan dust/aerosols over the Cape Verde Islands (CVAO = Cape Verde Atmospheric Observatory) is described by Fomba et al. (2014).

3 Material and methods

3.1 The Cape Verde Ocean Observatory (CVOO)

The in situ observations used in this study have been acquired at the Cape Verde Ocean Observatory (CVOO), located in the eastern tropical North Atlantic (17°35′ N, 24°15′ W, Fig. 1) ca. 800 km west of the African coast and about 80 km north of the Cape Verde Islands. The site consists of a deep-sea mooring (3600 m water depth) that was first deployed in September 2006 and is operational since then. The sediment trap data discussed here were acquired at two depths during the deployment period October 2009 to May 2011 (CVOO-3). The mooring is equipped with a set of core sensors for hydrography (temperature, salinity sensors at different depth), currents (profiling in upper 100 m and single RCM-8 instruments at approximately 600, 1300, and 3400 m depth), and oxygen (typically 2 single sensors at 50 and 180 m depth). For analysis of the currents, we considered data from the CVOO-3 period with one current meter at 588 m, one at 1320 m (30 m below the upper trap), and the deepest at 3473 m (46 m below the lower trap). For the 588 m and the upper trap RCM, complete time series of speed and direction are available. For the lower trap RCM, because of a rotor failure, only current direction but no current speed is available after mid December 2009. RCM-8 current meters have a speed threshold < 2 cm s^{-1} and measure speed with ±1 cm s^{-1}

BGD
12, 18253–18313, 2015

or 2% of measured speed (whatever is larger). Speed data $< 1.1\,cm\,s^{-1}$ has been set to the threshold of $1.1\,cm\,s^{-1}$. Compass accuracy is ±7.5° for speed $< 5\,cm\,s^{-1}$ and 5° above that threshold.

3.2 Sediment traps and bulk particle fluxes

Particle fluxes were aquired using two classical cone-shaped and large-aperture sediment traps ($0.5\,m^2$; Kiel type, Kremling et al., 1996) which were moored at the CVOO site (Karstensen et al., 2015a), The trap depths were in 1290 and 3439 m, respectively. We collected sinking material with bathypelagic traps to circumvent flux biases such as undersampling due to strong ocean currents and/or zooplankton activities (e.g. Buesseler et al., 2007, for a review). It is known that trapping efficiency is best at water depths > 1200 m water depths (see summary in Boyd and Trull, 2007; Berelson, 2002; Yu et al., 2001). We used samples collected on roughly monthly intervals (each 29 days) during the period between December 2009 and March 2011. Detailed sampling periods are given in Table 1, together with the bulk mass fluxes and relative composition of the particles. The traps were equipped with 20 cups, which were poisoned with $HgCl_2$ before and after deployment by addition of 1 mL of a saturated $HgCl_2$ solution in distilled water at 20 °C per 100 mL. Pure NaCl was used to increase the density in the cups prior to the deployments (final salinity was 40 ‰). Large swimmers were removed manually, and other swimmers were removed by filtering carefully through a 1 mm sieve. Thus, all fluxes refer to the size fraction of < 1 mm. Flux of the size fraction of particles > 1 mm was negligible. Samples were wet-split in the home laboratory using a rotating McLANE wet splitter and subsequently freeze-dried. For a detailed description of the methods see Fischer and Wefer (1991).

Sediment trap samples were analyzed using freeze-dried homogenized material of 1/5 wet splits. It was weighed for total mass and analysed for organic carbon, total nitrogen, carbonate and biogenic silica. Particulate organic carbon, total nitrogen and calcium carbonate were measured by combustion with a Vario EL III Elemental Analyzer in

BGD
12, 18253–18313, 2015

the CN mode. Organic carbon was measured after removal of carbonate with 2 N HCl. Overall analytical precision based on internal lab standards was 2.8033 % ± 0.0337 for organic carbon and 0.3187 % ± 0.0082 for nitrogen, respectively. Carbonate was determined by subtracting organic carbon from total carbon, the latter being measured by combustion without pre-treatment with 2 N HCl. Biogenic opal was determined with a sequential 1 M NaOH-leaching method according to Müller and Schneider (1993). The precision of the overall method based on replicate analyses is between ±0.2 and ±0.4 %. Lithogenic fluxes were calculated from total mass flux by subtracting the flux of carbonate, biogenic opal and two times the flux of TOC to approximate organic matter.

Deep ocean sediment traps collect material from a rather large catchment area, typically around 100 km in diameter or wider, depending on particle settling rates and ocean currents (Siegel and Deuser, 1997). Making use of current meter data records from the upper water column (600 and 1300 m), the progressive vector diagrams (PVD) (Fig. 2) show that the collected material before the eddy passage was under the impact of a current from the NE, while after the eddy passage the material was transported more from the southwest. In general, the currents are about twice as strong in 600 m compared to the 1300 m depth and remained mostly below 10 cm s^{-1}.

3.3 Siliceous phytoplankton studies

For this study, 1/125 splits of the original samples were used. Samples were rinsed with distilled water and prepared for siliceous plankton studies following the method proposed by Schrader and Gersonde (1978). Qualitative and quantitative analyses were done at x1000 magnifications using a *Zeiss*® Axioscop with phase-contrast illumination (MARUM, Bremen, Germany). Counts were carried out on permanent slides of acid cleaned material (*Mountex*® mounting medium). Depending on diatom valve abundances in each sample, several traverses across each slide were examined. The total number of counted valves ranged between 300 and 600. At least two cover slips per sample were scanned in this way. Diatom counting of replicate slides indicates that

BGD
12, 18253–18313, 2015

the analytical error of the concentration estimates is ≤ 15 % (Schrader and Gersonde, 1978).

The resulting counts yielded abundance of individual diatom taxa as well as fluxes of diatom valves per $m^{-2}\,d^{-1}$ calculated according to Sancetta and Calvert (1988), as follows:

$$F = \frac{[N] \times [A/a] \times [V] \times [\text{Split}]}{[\text{days}] \times [D]}$$

where, [N] number of valves, in an area [a], as a fraction of the total area of a petri dish [A] and the dilution volume [V] in mL. This value is multiplied by the sample split [Split], representing the fraction of total material in the trap, and then divided by the number of [days] of sample deployment and the trap collection area [D].

3.4 Coccolithophores studies

For coccolith counts, wet split aliquots of each sample (1/25 of the < 1 mm fraction) were further split by means of a rotary sample divider (Fritsch, Laborette 27) using buffered tap water as the split medium. Studied splits ranged between 1/250 and 1/2500, which were filtered onto polycarbonate membrane filters (Schleicher and Schuell TM 47 mm diameter, 0.45 µm pore size). The filters were dried at 40 °C at least for 12 h before a randomly chosen small section of the filter was cut out and fixed on an aluminium stub, sputtered with gold/palladium. The coccolith analysis was carried out using a scanning electron microscope (Zeiss DSM 940A) at 10 kV accelerating voltage. In general more than 500 coccoliths were counted on measured transects at a magnification of 3000×.

3.5 Calcareous zooplankton studies

The mass flux of carbonate is mainly constituted of planktonic foraminifera, pteropods and nanofossils/coccolithophores. To determine the proportion of calcareous zooplankton, a 1/5 split of the < 1 mm fraction was used to pick planktonic foraminifera and

BGD
12, 18253–18313, 2015

pteropods from the wet solution. The picking was done by hand with a pipette under a ZEISS Stemi 2000 microscope. Picked shells were rinsed three times with fresh water and dried at 50 °C overnight. Total mass fluxes of pteropods and planktonic foraminifera were determined with a Sartorius BP 211D analytical balance and mass fluxes ($mg\,m^{-2}\,day^{-1}$) were calculated. The foraminiferal species composition was determined under a ZEISS V8 microscope. The fluxes of all species were calculated and displayed as individuals per m and day.

3.6 Stable nitrogen isotope ratios

For the determination of the $\delta^{15}N$ of organic material, about 5 mg of freeze-dried and homogenized material was used. The $\delta^{15}N$ was measured at the ZMT (Leibniz Center of Tropical Marine Ecology, Bremen). The Delta plus mass spectrometer is connected to a Carlo Erba Flash EA 1112 (Thermo Finnigan) elemental analyzer via a Finnigan ConFloII interface. Helium carrier gas constantly flows to the EA, ConFloII, and mass spectrometer. Samples are combusted in an enriched oxygen environment in the combustion/oxidation column producing CO_2, N_xO_x, SO_2, and H_2O. The combustion/oxidation column, reduction column, and water trap work in series to insure that only N_2 and CO_2 enter the GC column and exit the EA. All of the data are expressed in the conventional delta (δ) notation, where the isotopic ratio of $^{15}N/^{14}N$ is expressed relative to air which is defined as zero. The N_2 reference gas we use is research grade and has been calibrated to air using IAEA-N1 and IAEA-N2. The internal standard used was pepton with a $\delta^{15}N$ value of 5.73 ± 0.07 ‰ (1σ).

3.7 Biomarker studies

For biomarker analyses, about 70–200 mg of freeze-dried and homogenized samples were extracted three times with dichloromethane (DCM) : methanol (MeOH) 9 : 1 (v/v) in an ultrasonic bath for 10 min. Internal quantification standards (squalane, 500 ng/nonadecanone, 499.5 ng/C_{46}-GDGT, 500 ng/erucic acid, 500.5 ng) were

BGD
12, 18253–18313, 2015

added prior the first extraction step. The solvent mixture was decanted and combined after each extraction step and following centrifugation. This total lipid extract (TLE) was dried under a gentle stream of nitrogen and saponified for 2 h at 80 °C using 1 mL of a 0.1 M KOH-solution in methanol : water (9 : 1). Following saponification, neutral lipids (NL) were extracted with 4 × 0.5 mL *n*-hexane. After acidification with HCl to pH < 2, fatty acids were recovered with 4 × 0.5 mL dichloromethane and esterified with methanolic HCl (12 h, 80 °C). Silica-gel chromatography was used to further separate NL. *n*-Hexane was used to elute a hydrocarbon fraction, *n*-hexane : DCM (2 : 1) for aromatic hydrocarbons, DCM : *n*-hexane (2 : 1) for ketones and DCM : MeOH (1 : 1) for polar compounds.

Alkenones were analyzed using a 7890A gas chromatograph (Agilent Technologies) equipped with an cold on-column (COC) injection system, a DB-5MS fused silica capillary column (60 m, ID 250, 0.25 µm film) and a flame ionisation detector (FID). Helium was used as carrier gas (constant flow, 1.5 mL min^{-1}) and the GC was heated using the following temperature program: 60 °C for 1 min, 20 °C min^{-1} to 150 °C, 6 °C min^{-1} to 320 °C and a final hold time of 35 min. Alkenone fractions were dissolved in *n*-hexane and the injection volume was 1 µL. Concentrations were calculated based on integrated peak areas and using the response factor of the internal standard (nonadecanone). The alkenone unsaturation index $U^{k'}_{37}$ was calculated as defined by Prahl and Wakeham (1987):

$$U^{k'}_{37} = \frac{C_{37:2}}{(C_{37:2} + C_{37:3})}$$

and converted to SSTs using the calibration of Conte et al. (2006).

$$T(°C) = -0.957 + 54.293\left(U^{k'}_{37}\right) - 52.894\left(U^{k'}_{37}\right)^2 + 28.321\left(U^{k'}_{37}\right)^3$$

The aromatic as well as the fatty acid methyl ester (FAME) fractions were analyzed by gas chromatography/mass spectrometry for the presence of isorenieratene and its derivatives and ladderrane fatty acids.

BGD
12, 18253–18313, 2015

4 Results

4.1 Mass fluxes

Mass fluxes increased in winter–spring 2009–2010 in both trap depths during the passage of the ACME at CVOO-3 but were rather low in winter–spring 2010–2011 (Fig. 3; Table 1). Fluxes were well correlated between both traps (r^2 = 0.6, N = 20), suggesting a fast transfer of the flux signature from the upper water column to bathypelagic depths. The deep trap flux was about twice as high as in the upper trap during the period of elevated fluxes in winter–spring 2009–2010. During winter 2010–2011, when no large eddy passed the study site CVOO, flux patterns showed only a small seasonal increase and the flux to the lower trap was lower in magnitude compared to winter–spring 2009–2010 (Fig. 3). We consider this as the "normal conditions".

The flux pattern of biogenic silica (BSi) showed a more discrete peak than total mass with maxima in February–March 2010 (Fig. 4a). BSi fluxes were highest in March for both traps and not in February when the ACME passed the study site. The high BSi fluxes arrived simultaneously at both trap depths without a time/cup lag between sampling depths. BSi fluxes were more than 3-fold higher in the deeper trap during February–March 2010 (Fig. 4a). Very low BSi fluxes were measured in winter–spring 2011 when no larger eddy passed and they were slightly higher in the upper trap level which is the common pattern. On an annual basis, the contribution of BSi to total flux mass was 2.8 % (upper) and 5.75 % (lower trap), respectively. However, during the ACME passage, the contribution increased significantly to 4.5–7.8 % (upper) and 8.3–12.3 % (lower trap) (Table 1). The opal fraction was mainly composed of marine diatoms. Organic carbon fluxes revealed a slightly different pattern from BSi with one distinct flux peak in February 2010 (Fig. 5a). Organic carbon fluxes in the deep trap were almost twice as high as those collected in the upper trap during February 2010. In contrast, during the "normal conditions" in winter–spring 2011, organic carbon fluxes showed only minor differences between the upper and lower traps.

BGD
12, 18253–18313, 2015

Lithogenic mass fluxes were more than twice higher in the deep trap during the period influenced by the ACME passage (Fig. 6) and followed organic carbon flux with a distinct peak in February 2010. In particular the deeper trap samples provided an almost perfect correlation between mineral dust and organic carbon fluxes (r^2 = 0.97, N = 17). This correlation was less pronounced for the upper trap samples (r^2 = 0.63, N = 18). As there is no river input in the study area, we assume that all non-biogenic (= lithogenic) material was supplied via atmospheric transport.

Total carbonate mass fluxes showed less seasonality than BSi and organic carbon with broad maxima in winter–spring 2009–2010, largely following total mass (Figs. 3–5 and 7). However, carbonate fluxes showed a decrease in February 2010 during the passage of the ACME, in particular in the deep trap. Fluxes of the major carbonate producers revealed a decrease in pteropod fluxes at both depths during February–March 2010. Planktonic foraminifera, however, showed a clear flux peak in the deep trap during February 2010 and a rather broad increase in the entire winter–spring 2009/10 at the upper trap (Fig. 7b). Total carbonate mass flux in winter–spring 2011 during "normal, non-eddy conditions" was much lower than in 2010 and decreased between the upper and lower trap, which is typical for years without eddy passage.

4.2 C/N- and δ^{15}N ratios

The molar C : N ratio of the organic material in both traps is rather high for deep ocean material compared to previous findings (Fischer et al., 2003, 2010). In February 2010, C : N ratios were unusually high with values around 18 and 25 in the upper and lower trap, respectively (Fig. 5b). The δ^{15}N ratios of the lower trap samples varied between 6.99 and 3.11 ‰ (Fig. 5c). The lowest value (3.11 ‰) was measured following the passage of the ACME in February 2010 while the highest value with almost 7 ‰ was recorded in December 2010. Distinct decreases were found from January to March 2010 (ACME passage), as well as from December 2010 to March 2011. The mean value was 4.16 ‰, the flux-weighted mean was with 3.98 ‰ slightly lower. The

BGD
12, 18253–18313, 2015

δ^{15}N ratios were not related to the C : N ratios nor to the fluxes of nitrogen and carbon in general.

4.3 Diatom fluxes

Biogenic silica flux showed a similar seasonal pattern as diatoms: a major peak occurred in the transition from late winter into early spring. The total diatom flux in the upper trap ranged from 2.3×10^3 to 1.7×10^5 valves $m^{-2} d^{-1}$ in the upper trap (Fig. 4b; Table 2). One major diatom flux maximum ($> 1.4 \times 10^5$ valves $m^{-2} d^{-1}$) occurred in mid-spring 2010. The opal fraction was mainly composed of marine diatoms. In addition, silicoflagellates, radiolarians, freshwater diatoms, phytoliths and the dinoflagellate *Actiniscus pentasterias* occurred sporadically. In terms of number of individuals, diatoms dominated the opal fraction throughout the year: their flux was always one to four orders of magnitude higher than that of the other siliceous organisms encountered (not shown here). The diverse diatom community was composed of ca. 100 marine species. The most important contributors to the diatom community were species typical of open-ocean, oligo-to-mesotrophic waters of the low and mid-latitude oceans: *Nitzschia sicula*, *Nitzschia bicapitata*, *Nitzschia interruptestriata*, *Nitzschia capuluspalae*, and *Thalassionema nitzschioides* var. *parva*. Resting spores of several coastal species of *Chaetoceros*, and tycoplanktonic/benthic *Delphineis surirella*, *Neodelphineis indica* and *Pseudotriceratium punctatum* are secondary contributors.

4.4 Coccolith fluxes

In general, both traps revealed coccolith fluxes that were high during the interval December 2009 to May 2010, whereas fluxes were considerably lower (ca. 2–10 times) during the rest of the studied period (Fig. 8a; Table 2). Maximum total coccolith fluxes were recorded in February 2010 for both traps, reaching values of 1300×10^6 coccoliths $m^{-2} d^{-1}$ (upper trap, Fig. 8a) and 2880×10^6 coccoliths $m^{-2} d^{-1}$ (lower trap, not shown), respectively. Total coccolith fluxes in the lower trap were gen-

BGD
12, 18253–18313, 2015

erally twice to three times higher than in the upper trap. In total, 56 coccolithophore species were identified. The coccolithophores were generally dominated by lower photic zone (LPZ) species, such as *Florisphaera profunda* and *Gladiolithus flabellatus*, together with more omnipresent species such as *Emiliania huxleyi* and *Gephyrocapsa* spp *Florisphaera profunda* constituted between 21.7 and 49.2% of the total assemblage and cosmopolitan *E. huxleyi* ranged between 13.4 and 29.4 %. Coccolith fluxes as well as %-abundances of *F. profunda* slightly decreased in January–March 2010, although this species shows a distinct flux peak in February (Fig. 8a). In contrast, fluxes of *E. huxleyi* as well as their relative proportion clearly increased during the interval February–March 2010 (Fig. 8a). Other taxa that considerably contributed to the assemblage are *Gephyrocapsa ericsonii* (2.3–16.7%), *G. oceanica* (0.9–6.7%), *G. muellerae* (0.3–14.0%) and *Umbilicosphaera sibogae* (1.1–6.7%), which all show a pattern generally similar to that of *E. huxleyi*. In contrast, deep-dwelling *G. flabellatus* (1.3–7.3%) and upper zone species *Umbellosphaera tenuis* (1.3–5.3%) tend to show less prominent fluxes in February 2010 during ACME passage. Other, more oligotrophic species (*U. irregularis, R. clavigera*) display a similar pattern.

4.5 Flux of planktonic foraminifera

Planktonic foraminifera showed a clear flux peak in February 2010 in the deep trap (not shown) and a rather broad increase over the entire winter–spring season in 2010 at the upper trap level (Fig. 7b; Table 2). The surface dwellers and warm water species *Globigerinoides ruber* white and pink and *Globigerinoides sacculifer* were the three dominant species to the total foraminifer flux in both the upper and the deeper trap throughout (Fig. 8b and c). In February 2010 during the passage of the ACME, however, all three species exhibit a decrease in occurrence. During this interval, they were replaced by the subsurface dweller *Globorotalia menardii*, dominating the foraminiferal flux at both trap levels (Fig. 8d, only upper trap shown). The deep dwellers were generally rare at the CVOO-3 site, either they were missing almost completely (*Globorotalia truncatulinoides*), or they were present in low numbers. *Globorotalia crassaformis,* for

BGD
12, 18253–18313, 2015

instance, showed a flux pattern with a maximum in April–May in both trap levels, following the ACME passage in February 2010.

4.6 Lipid biomarkers

A reduced sample set from the upper trap, covering the sample period from December 2009 to July 2010 (samples #1–8), was used for investigation of the organic biomarker composition and the characterization of the ACME passage. Alkenone-derived $U^{k'}_{37}$ values, a biomarker based proxy for SSTs, varied from 0.82 to 0.98 with the minimum value occurring in March, following the ACME passage (Table 3). Translation of the index into absolute temperatures by using the Conte et al. (2006) global calibration for surface particulate matter resulted in SSTs from 23.6 to 28.0 °C (Fig. 9a). From December 2009 to end of March 2010, SSTs decreased from 26.5 to 23.6 °C. After the ACME passage, starting in April 2010, SSTs shifted back to around 28.0 °C. Alkenone fluxes (Fig. 9a) showed a distinct 6 to 8-fold increase during ACME passage and correlate with organic carbon flux (Fig. 5a) and the molar C : N ratios of organic matter (Fig. 9b, $r^2 = 0.77$, $n = 8$). The relationship between alkenone and total coccolith fluxes, however, is weak (Figs. 8a and 9). Unique membrane lipids of anammox bacteria, so-called ladderanes (Sinninghe Damsté et al., 2002) nor biomarkers related to a pigment of the photosynthetic green sulphur bacteria *Chlorobiaceae*, isorenieratene and its derivatives, all indicative of photic zone anoxia, could not be detected.

5 Discussion

5.1 Production and export within the surface layer of the eddy

The upper CVOO-3 trap revealed a rather unusual high BSi flux in winter–spring (around 4 mg m^{-2} d^{-1}; Fig. 4a) which was partly higher than at the more coastal and mesotrophic Cape Blanc site CB (Fischer et al., 2003). The latter site is located within

BGD
12, 18253–18313, 2015

the "Giant Cape Blanc filament" that is characterized by high chlorophyll streaming offshore (Van Camp et al., 1991; Helmke et al., 2005). We argue that the unusual high BSi flux during the eddy passage was due to BSi and diatom production within the surface waters of the ACME. The diatom flux pattern revealed a distinct increase in February 2010 with a major peak later in early spring (Fig. 4b). The thermocline shoaled from about 50–60 m before the passage of the eddy to about 20 m in February 2010 during the eddy passage at CVOO (Karstensen et al., 2015a). Elevated chlorophyll and primary production within the eddy is seen from selected chlorophyll maps (Fig. 1) and has been discussed in the context of upward nutrient fluxes, particularly associated with ACMEs (e.g. Karstensen et al., 2015a; Benitez-Nelson and McGullicuddy, 2008). Considering the distinct BSi flux signal, this may indicate that the organic carbon is primarily fixed on the western side of the eddy where the most intense bloom is expected (Chelton et al., 2011). Sargasso Sea ACMEs, for instance, contain significant numbers of diatoms, regardless of the age of the eddy (McNeil et al., 1999; Sweeney et al., 2003; Ewart et al., 2008). The upwelling of nutrients within the eddy is driven by submesoscale processes, which are highly variable in space and time. As such, pulsed nutrient/silicate injections from subsurface waters probably combined with a high regeneration of nutrients within the upper layer are likely to occur. The BSi flux data support these findings and further suggest some vertical transport of nutrients (from the silicate-richer water of the shadow zone region east of the CVFZ) into the photic zone of the eddy in the beginning of 2010. In addition, protection of the organic materials in the diatom valves while sinking through the low-oxygen zone of the eddy may have contributed to elevated BSi fluxes in the deep ocean due to reduced BSi dissolution (Ragueneau et al., 2000).

The molar C : N ratios of organic matter were unusually high in February 2010 for both trap samples (Fig. 5b). They clearly fall far off the range of deep-ocean sediment trap samples or surface sediments with partly degraded organic marine material (C : N around 8–10; Fischer et al., 2003, 2010; C : N= 5–10; Tyson, 1995; Wagner and Dupont, 1999). The area of Cape Verde is influenced by wind-transported

BGD
12, 18253–18313, 2015

material which also contains some terrestrial organic matter with elevated C : N values (global mean = 24; Romankevich, 1984), clearly above the marine signal (e.g. Müller, 1977; Wagner and Dupont, 1999). This terrestrial organic matter is mixed with the debris of major marine primary producers (e.g. diatoms, coccolithophores) whose C : N values are around the Redfield Ratio (Redfield et al., 1963; Martiny et al., 2013). The exceptionally high ratios in February 2010 (C : N= 18 (upper) and 25 (lower trap) (Fig. 5b), however, cannot be explained by mixing processes of marine and terrestrial organic materials alone, because this would suggest a preferential contribution of terrestrial organic matter. Nitrogen (nitrate) limitation in the generally oligotrophic setting north of the Cape Verde Islands must be taken into account to explain the high C : N ratios of organic matter (e.g. Laws and Bannister, 1980; Martiny et al., 2013; Löscher et al., 2015a). We have to consider that production within the surface eddy was sometimes characterized by low growth rates of the primary producers (both diatoms and coccolithophores), combined with a reduced nutrient availability, e.g. in January/February 2010. This process could explain the extraordinary high C : N ratios (Laws and Bannister, 1980; Martiny et al., 2013) in February 2010.

Nitrogen limitation is also known to increase the C : N ratios of the alkenone producers (e.g. Löbl et al., 2010), and might result in an increase in the production and storage of alkenones (e.g., Eltgroth et al., 2005; Prahl et al., 2003). Alkenone temperature records from the Subtropical Front at the Chatham Rise, SW Pacific Ocean (Sikes et al., 2005) showed that biases occurred during times of highest lipid fluxes and low nutrient conditions in the surface mixed-layer. When plotting the C : N ratios versus the alkenone fluxes of the upper trap samples, we indeed obtain a relationship (Fig. 9, $r^2 = 0.77$, $n = 8$) which could point to nutrient limitation during or shortly before the ACME passage. Our temperature record derived from the unsaturation index of the alkenones revealed a stepwise decrease in SST by about 2 °C (Fig. 9a) from December 2009 to March 2010. However, these changes are not very much different from the general seasonal SST changes derived from satellite observations (Fig. 9a).

BGD
12, 18253–18313, 2015

The scenario of nutrient limitation within the surface water of the eddy at some time is supported by elevated fluxes of BSi and organic carbon in February–March 2010 and agrees with a decrease of chlorophyll between November/December 2009 and again between January/February 2010 as shown in satellite ocean color maps (Fig. 1). However, we have to consider that our time resolution of the sampling cups is rather low (29 days) and our traps thus may not capture the highly dynamic biogeochemistry within the eddy and the resulting export fluxes which may fluctuate within days and weeks. Secondly, variable settling rates of different larger particles produced in the surface and subsurface waters of the eddy make it difficult to estimate the variable time lags between the arrival of the flux signature in the bathypelagic traps and the responsible processes in the surface and subsurface waters.

The δ^{15}N ratios of the deep trap samples revealed a stepwise decrease in winter 2009/10 (5.21 to 3.11 ‰) during the passage of the ACME and during winter 2010–2011 as well (6.99 to 3.45 ‰) (Fig. 5c). The general pattern of δ^{15}N did not reveal any overall relationship between δ^{15}N ratios and nitrogen or organic carbon fluxes (Fig. 5a and c), as for example described for the oligotrophic Sargasso Sea (BATS, Altabet and Deuser, 1985). These authors found low δ^{15}N ratios (around 0 ‰) during times of highest organic carbon fluxes and elevated ratios (up to 3 ‰) at low fluxes. For the coastal upwelling in the Benguela Current, Holmes et al. (2002) observed a similar relationship between fluxes and δ^{15}N ratios. At CVOO-3, nitrogen and carbon fluxes increased and the δ^{15}N ratios decreased (Fig. 5) when the eddy passed the CVOO site. During the following non-eddy winter, δ^{15}N was high at the end of 2010 (almost 7 ‰) at slightly elevated N-flux, later decreasing with decreasing fluxes. Thus, there is no exceptional δ^{15}N pattern during the approach and passage of the ACME in 2010.

δ^{15}N ratios of settling particles are mainly dependent on the source water δ^{15}N of nitrogen species utilized by the primary producers, in most cases, nitrate (Ryabenko et al., 2012; Altabet and Deuser, 1985). More specifically, the isotope ratio reflects the degree of nitrate utilization (Mariotti et al., 1982), rather than absolute nitrate concentrations. Values of DIN in the OMZs of the Atlantic were 5.4 ‰ on average, those from

BGD
12, 18253–18313, 2015

AAIW around 5.5 ‰ (Ryabenko et al., 2012), both close to global averages (Liu and Kaplan, 1989). Phytoplankton preferentially takes up the lighter isotope during photosynthesis (e.g. Altabet et al., 1991), leaving the remaining nitrate pool enriched in ^{15}N. In general, $\delta^{15}N$ is high in temperate oceans after nitrate is depleted due to phytoplankton growth and low in more stable, oligotrophic seas (Saino and Hattori, 1987). Our $\delta^{15}N$ record in winter–spring 2009–2010 may reflect episodic nutrient injection into the euphotic zone of the ACME (Karstensen et al., 2015b), leading to increased particle formation and fluxes documented in February–March 2010 in the lower trap (Fig. 5c). This nutrient injection from below can be deduced from a stepwise cooling starting in January 2010 and ending in March, as seen in the record (Fig. 9a) The higher N-fluxes were associated with a lowering of $\delta^{15}N$ as expected from other studies. The relatively high $\delta^{15}N$ value of 5.21 ‰ in January 2010 (Fig. 5c) shortly before the ACME passage could document some depletion in nitrate which may also explain the unusually high molar C : N ratios (18–25) one month later (Fig. 5b).

Under low oxygen conditions, denitrification by nitrate-reducing bacteria can affect the isotopic signature of the nitrate pool, leading to a significant enrichment of ^{15}N in the residual nitrate pool relative to a deep water value of around 6 ‰ (Liu and Kaplan, 1989; Libes and Deuser, 1988). Our generally higher $\delta^{15}N$ ratios compared to the oligotrophic Sargasso Sea (Altabet and Deuser, 1985) may be partly explained by the injection of ^{15}N enriched source waters within the ACME. From high resolution nitrate/oxygen survey in low oxygen eddies, Karstensen et al. (2015b) have clear indications for local nutrient recycling in the upper 200 m. A rapid remineralization of the sinking material releases dissolved nitrate to shallow depth, which is then returned to the surface layer by sub-mesoscale driven processes in association with ACMEs. Nitrate becomes part of the sinking material but oxygen not. As a consequence, dissolved nitrate is enriched while oxygen is consumed. As the AMCE is over the typical oxygen threshold that support the onset of denitrification, it is not unlikely that denitrification in the eddy leads to more positive $\delta^{15}N$ in the nitrate source waters (Liu and Kaplan, 1989). Löscher et al. (2015b) found transcription of the key gene for denitrification in

BGD
12, 18253–18313, 2015

a low oxygen ACME in the Cape Verde region studied in 2014. In the Arabian Sea, for instance, source waters had values around 6–10% due to denitrification (e.g. Schäfer and Ittekkot, 1983).

The vertical distribution of many coccolithophore species is often controlled by upper photic-zone temperature and water stratification (e.g. Jordan and Chamberlain, 1997; Hagino et al., 2000). In particular, *E. huxleyi* is known to preferentially thrive in more turbulent and nutrient-enriched waters as found in upwelling areas or coastal regions (e.g., Haidar and Thierstein, 2001; Hagino and Okada, 2006; Boeckel and Baumann, 2008). Thus, the increasing fluxes during February–March 2010 (Fig. 8a) correspond well to nutrient-enriched conditions during this time interval or somewhat before. Alkenones, synthesized by planktonic algae such as coccolithophorids show a peak in flux during this time interval (Fig. 9). These observations correspond to nutrient measurements conducted in the low oxygen ACME in 2014 (Fiedler et al., 2015). The coccolithophore flora in the upper photic zone (UPZ) down to about 40–60 m is often composed of *Umbellosphaera tenuis, U. irregularis,* and *Discosphaera tubifera*, adapted to warm temperatures and low nutrient levels (e.g., Honjo and Okada, 1974; Hagino et al., 2000; Malinverno et al., 2003; Boeckel and Baumann, 2008). The same pattern is displayed by *Rhabdosphaera clavigera*, *R. stylifer* and *Syracosphaera pulchra*, all of which are non-placoliths known to prefer stable stratified waters (Hagino et al., 2000). All these latter three species show a rather similar pattern with slightly increased fluxes in February–March 2010 when the ACME passed. The species *F. profunda*, *G. flabellatus* are well established as species belonging to the lower-photic zone community (e.g., Honjo and Okada, 1974; Takahashi and Okada, 2000; Andruleit et al., 2003). In particular, *F. profunda* is known to occur exclusively in the deep photic zone (ca. 40–200 m), typically occurring at maximum abundances below the deep chlorophyll maximum in relatively high abundances (Haidar and Thierstein, 2001). During the ACME passage, we observed an increase in coccolith fluxes in February–March 2010 (Fig. 8a) and slightly less contribution of deeper dwelling species such as *F. profunda and G. flabellatus,* probably due to the suboxia/hypoxia in the deeper water where

BGD
12, 18253–18313, 2015

these species thrive. However, a clear impact of the low oxygen conditons in the ACME on the photosynthetic coccolithophore community cannot be observed.

5.2 Origin of hypoxia/suboxia and organic matter preservation within the eddy

Neither the diatom nor the coccolithophore communities do show any significant coastal influence in the collected materials. Given the ocean currents to the south-west and the proximity to the NW African coast, it is not unreasonable to suspect that diatom blooms above the CVOO mooring may have been due to a seed population from coastal waters. The diatom assemblage, however, shows no signature of coastal upwelling and benthic diatoms, as indicators of entrained coastal waters. Low relative contributions of coastal upwelling-related resting spores of *Chaetoceros* (Romero et al., 2002) and a few benthic species, which thrive in near-shore waters above 50 m water depth (Round et al., 1990; Romero et al., 2015), suggests weak transport of plankton communities from near-shore/coastal waters into the pelagial north of the Cape Verde Islands. This east-to-west seaward transport did not carry substantial amounts of microorganisms nor did it vastly contribute to the pool of nutrients in waters overlying the CVOO site. Further evidence is provided by the coastal : pelagic ratio of the diatom assemblage of the upper trap (Fig. 4c). Compared to the values recorded at 200 nm off Cape Blanc (Mauritania, CB trap site), the coastal : pelagic ratio of 20 to 25 at CVOO-3 is lower than values recorded at the CB site. At all times, the dominance of oceanic species at the CVOO-3 site reveals in situ diatom production with minor transport from the coastal realm. This indicates that the eddy at the time of its passage at CVOO-3 had significantly altered since its origin at the African coast at around 18° N in summer 2009 (Karstensen et al., 2015). At the origin of the ACME in summer 2009 off the West African coast, suboxia had not existed and oxygen was between 40 and 70 $\mu mol\,kg^{-1}$ in the depth range of the later suboxic/hypoxic zone (40–170 m) in February 2010 (Karstensen et al., 2015a). The severe suboxia/hypoxia in February 2010 therefore developed en-route between summer 2009 and winter 2010. From satellite chlorophyll imagery (Karstensen et al., 2015a) and high resolution MODIS

BGD
12, 18253–18313, 2015

data, the ACME approaching the CVOO site showed a decrease in chlorophyll between November/December 2009 and January and again between January and February 2010 (Fig. 1). In February 2010, only an unclear and ring-like structure of slightly elevated but still rather low chlorophyll of approximately the size of the ACME remained within the oligotrophic surrounding area (Fig. 1a). However, a general high cloud cover renders satellite-based estimates difficult. The elevated C : N ratios in February 2010 found at both trap depths suggest some nutrient limitation followed by slow growth rates of phytoplankton (e.g. Laws and Bannister, 1980; diatoms and coccolithophores) in the productive surface layer at the beginning of 2010 (see Sect. 5.1.). This could indicate that sedimentation of biogenic detritus started around the transition 2009–2010, matching the maxima of fluxes in February–March (Figs. 3–5). Using conservative estimates of particle settling rates (200 m day^{-1}), about 1–3 weeks are needed for larger particles to travel down to the bathypelagic traps. The sinking detritus from the surface production was likely to have contributed to the low oxygen within the ACME as suggested by Karstensen et al. (2015a). Considering the chlorophyll decrease at the transition 2009–2010 (Fig. 1), we assume that the severe suboxia within the eddy originated around the turn of the years 2009–2010 due to particle remineralization. During the passage of the westward moving eddy, high chlorophyll standing stocks could be noticed until the beginning of January 2010 (Karstensen et al., 2015), which should lead to the formation of larger settling particles. These organic-rich particles could have reduced oxygen concentrations within the westward moving eddy until the turn of 2009–2010.

Screening of the samples #1–8 of the upper trap for the presence of unique membrane lipids of anammox bacteria, so-called ladderanes (Sinninghe Damsté et al., 2002) did not provide evidence for the presence of such compounds during the ACME passage. Further, we could not detect biomarkers related to a pigment of the photosynthetic green sulphur bacteria *Chlorobiaceae*, isorenieratene and its derivatives, all indicative of photic zone anoxia (e.g. Koopmans et al., 1996). Bacterial communities detected in OMZs including green sulfur bacteria and anammox bacteria (see summary in Löscher et al. (2015a) were not found with the analysis of lipids. However,

BGD
12, 18253–18313, 2015

detection of these compounds requires the respective bacterial stocks to be present in concentrations above a certain detection threshold and/or an effective export mechanism for them leading to incorporation into sinking particles. Although one might expect these compounds to be present during the ACME passage when low oxygen conditions prevailed in the subsurface waters (Löscher et al., 2015a), likely the populations of the organisms have not reached significant levels, because suboxic conditions just recently developed within the eddy. Another possible explanation is that the above mentioned bacteria were present in the suboxic zone of the eddy, but did not interact and were not attached to the fast sinking organic-rich particles which originated in the surface layer and later constituted the mass flux.

No signs of dissolution in sinking calcareous particles i.e. coccolithophores or foraminifera are seen, which might have occurred due to reduced pH within the suboxic/hypoxic parts of the eddy. The low oxygen ACME waters surveyed in 2014 had a pH of about 7.6 (Fiedler et al., 2015). No signs of carbonate dissolution could either point to a rapid transport of sinking carbonate particles through the suboxic/hypoxic water column of the ACME as outlined above or to some protection of carbonate particles by periotrophic membranes of fecal pellets or both.

5.3 Mineral dust and particle settling rates

In general, both traps revealed similar flux signals with maxima around February to March 2010 (Figs. 3–5) and coinciding with the passage of the ACME with elevated biomass in the surface ocean over the CVOO-3 site (Fig. 1). Considering the synchronicity of peaks in BSi and other components, a fast vertical transport of the surface particle flux signature into the meso- and bathypelagic is expected within the eddy. Given the 29 day sampling interval of the traps, the particle settling rate for the bathypelagic water column should at least $150\,\mathrm{m\,d^{-1}}$, applying the methods described in Fischer and Karakas (2009) and Berelson (2002). Fischer and Karakas (2009) provided a compilation of particle settling rates with a mean of $235 \pm 71\,\mathrm{m\,d^{-1}}$, using several particle flux patterns from the mesotrophic Cape Blanc moorings, located directly in

BGD
12, 18253–18313, 2015

the EBUEs and much closer to the coast. For the sediment trap mooring sites south of the Cape Verdes (CV 1-2), an even higher mean sinking speed of 416 m d^{-1} was estimated (Fischer and Karakas 2009). The authors argued that high organic carbon fluxes in the CC compared to other EBUEs are at least partly due to high particle settling rates which result in low carbon respiration rates (Iversen and Ploug, 2010), most probably favored by a high ballast content such as mineral dust.

Deep trap organic carbon fluxes plotted versus the fluxes of mineral dust provided an exceptionally good empirical relationship (r^2 = 0.97; N = 17, Fig. 7) which we never observed before off NW Africa (e.g. Fischer et al., 2010). This relationship, however, does not explain the complex processes involved in the formation of larger and fast sinking settling particles in the surface and subsurface waters and the interaction of biogenic with non-biogenic particles. Lab experiments with roller tanks and ballast minerals, however, clearly indicate the importance of mineral ballast for increasing sinking rates and lower carbon degradation within marine snow aggregates (Ploug et al., 2008; Iversen and Ploug, 2010). Additional evidence is provided by observations gained during a field campaign in winter 2012 off Cape Blanc (eutrophic site CBi): higher organic carbon fluxes at 100 and 400 m water depths using drifting traps were recorded, matching faster particle settling rates after a 1–2 days, low altitude dust storm event (Iversen et al., 2015).

Besides the question of the development of suboxia/hypoxia within the eddy discussed above, the causes of enhanced sedimentation of biogenic detritus in February–March are unclear. From our field studies in the Cape Blanc area (e.g. Fischer and Karakas, 2009) and lab studies with in situ chlorophyll and mineral dust (e.g. Iversen, unpubl.; van der Jagt, unpubl.), we speculate that Saharan mineral dust which preferentially settles in winter in the Cape Blanc and Cape Verde ocean area (e.g. Gama et al., 2015) could have contributed or even initiated particle settling via ballasting of organic-rich aggregates (Ploug et al., 2008; Iversen and Ploug, 2010; Iversen and Robert, 2015) produced within the chlorophyll enriched eddy. Some effect on particle produc-

BGD
12, 18253–18313, 2015

tion and fluxes by fertilization due to the input of macro-nutrients by dust (e.g. nitrogen; Fomba et al., 2014) via dust cannot be excluded.

Fluxes of organic carbon and mineral dust co-varied (Fig. 6) which means that both components settled in close association into the bathypelagic. In the high dust region south of the Cape Verdes, Ratmeyer et al. (1999) obtained correlation coefficients of ca. 0.6 between dust and organic carbon in the deep traps. Time-series of aerosol optical thickness (AOT, 869 nm, 9 km resolution) from MODIS did show unexpectedly high values for dust concentration in the atmosphere above a 1 or 4° grid over the CVOO site in early 2010. However, the AOT did not provide a true dust deposition rate at the ocean surface in winter 2010 at the study site. At the Cape Verde Islands, Fomba et al. (2014) and Gama et al. (2015) found highest aerosol/dust concentrations during winter with distinct peaks between January and March when the eddy with increased chlorophyll and primary production approached and passed the CVOO site. However, extraordinarily high dust concentrations early in 2010 were not recorded (Fomba et al., 2014). We assume that some dust deposition at the ocean surface combined with elevated chlorophyll within the eddy, could have resulted in the particle flux signature in February–March 2010.

By comparing the fluxes in winter–early spring 2009–2010 under the influence of the ACME and the suboxia/hypoxia with winter–early spring 2011, when no larger eddy passed the CVOO site, the contribution of the ACME to annual mass flux can be estimated. This estimation does not consider interannual variability of absolute mass fluxes nor changes in seasonality/timing of maxima from year-to-year and therefore has to be regarded as a first estimation. When comparing the organic carbon fluxes of the upper trap for the first four months of both years, we roughly obtain a three-fold increase in carbon flux when the eddy passed over the CVOO site compared to an eddy-free year (Fig. 5a). These estimates match rather well with data determined in the low oxygen ACME in 2014 (Löscher et al., 2015b). These authors obtained chlorophyll concentrations and carbon uptake rates within the eddy of up to three times as high as in the surrounding waters.

BGD
12, 18253–18313, 2015

5.4 Differences of fluxes in the water column

There is a significant increase in mass fluxes with depth from December 2009 to May 2010, a common feature of many ocean areas, in particular at near-continental margins sites (e.g. Neuer et al., 2002; Honjo et al., 2008; Fischer et al., 2009b). At the open ocean site CVOO-3, however, the organic carbon fluxes were more than twice as high in the deep trap compared to the upper trap and correlated with $r^2 = 0.70$. BSi flux was more than three-fold higher at greater depth (correlated coefficient $r^2 = 0.91$) during the eddy passage. The flux of coccoliths increased with depth by three-fold was well. For organic carbon, an overall decrease in flux with depth has to be expected (when excluding lateral advection), following an exponential equation in classical oceanic settings with sufficient oxygen in the water column (see summary in Boyd and Trull, 2007). As pointed out by Siegel and Deuser (1997), deeper traps have a larger catchment area than shallower ones and may sample additional material from lateral sources like a statistical funnel. Assuming a rather conservative settling rate of 200 m d^{-1} for particles with high ballast content (see Fischer and Karakas, 2009), we obtain catchment areas with a length scale of around 300 km for the upper trap and 400 km for the lower one when using particle trajectories from the Sargasso Sea (Siegel and Deuser, 1997).

The mean currents at the CVOO site were sluggish with monthly mean velocities between 2 to 6 cm s^{-1} (equivalent to 1.5 to 5.1 km day^{-1}) for the upper trap and up to 2 cm s^{-1} (1.7 km day^{-1}) for the lower trap, considering the velocity data from CVOO-2 (March 2008 to October 2009, not shown here) and CVOO-3. These currents will primarily add a displacement of the sinking particles that results in a difference between the particle source areas of the two sediment traps (Siegel and Deuser, 1997). The gravitational sinking speed has been found to vary over a wide spectrum but it is likely that in our study area values of several hundred of meters per day are reached (e.g. Fischer and Karakas, 2009). In case of a settling rate of 100 m day^{-1} and sluggish lateral flux (2 km day^{-1}), the setting of a particle through a 3500 m water column will take

BGD
12, 18253–18313, 2015

about 35 days and the material is displaced by less than 100 km. For interpreting the flux data, the origin of laterally derived particles and hence the prevailing flow direction is of particular importance. High chlorophyll is found in the coastal upwelling off West Africa approximately 300 to 700 km away from CVOO (Fig. 1). Comparing the progressive vector diagrams (PVD) from three depth at CVOO-3 for the period December 2009 to May 2010 it is evident that the upper trap (Fig. 2b) is primarily under the impact of meridional transport from the south and also reflected in the thermocline transport (Fig. 2a), while the lower trap is more under zonal transport from the east (Fig. 2c). However, because of the rotor failure it is unclear how far the catchment in the lower trap is extending. As expected, during the eddy passage all three RCMs show varying currents dominated by the local circulation associated with the eddy. The nearest and most probable additional particle source area for the deep CVOO-3 trap to the east and northeast is the approaching ACME at a time when chlorophyll, production and export to deeper waters was higher than in February 2010, e.g. in November/December 2009 and in early January 2010 (Fig. 1). This additional material could be laterally transported to the deep trap by the prevailing current system (Fig. 2c), thus enhancing the deep bathypelagic fluxes by a factor of two to three in winter–spring 2010.

5.5 Zooplankton within the eddy and organic carbon degradation

Acoustic backscatter data from Karstensen et al. (2015a) suggest that at least some zooplankters stopped their diel vertical migration behavior when the suboxic part of the eddy approached the CVOO site around February 2010. This seems to be typical for open ocean OMZ (Ayon et al., 2008). Mobile zooplankton such as certain copepods escape from oceanic dead zones (e.g. the ACME 2010), while certain less mobile protozoa such as planktonic foraminifera, may be encountered by the suboxia, die and settle down. In a low oxygen eddy observed in spring 2014 at CVOO, acoustic backscatter data and multinet sampling indicated a compression of zooplankters in the surface waters with a high abundance of calanoid copepods and euphausiids (Hauss

BGD
12, 18253–18313, 2015

et al., 2015). This suggests a high grazing pressure on these organisms in the surface layer during eddy passage.

The flux patterns of planktonic foraminifera revealed a clear peak flux in February 2010 in the lower trap, matching the passage of the suboxic eddy. The subsurface (50–100 m water depth) dweller *Globorotalia menardii* largely responsible for this flux peak in the upper trap in February 2010 (Fig. 8d), is a tropical to subtropical, non-spinose species with changing depths habitats (Hemleben et al., 1989). We assume that the oxygen within the ACME became too low in early 2010 and the more or less immobile *G. menardii* died , resulting in sedimentation and elevated fluxes in both trap levels. Foraminifera are generally assumed to settle with high rates of several hundreds to a few thousand meters per day (Kucera, 2007), thus, a clear flux signal without time delay is expected in the two bathypelagic traps. The near-surface dwellers *Globigerinoides ruber pink* and *white* and *Globgerinoides sacculifer,* on the other side, showed a clear decline in flux in February 2010 in both trap samples (Fig. 8b and c), contributing to reduced total carbonate fluxes (Fig. 7). This pattern might be due to the shoaling of the thermocline from 50–60 m to about 20 m (Karstensen et al., 2015a) and a decrease in SST (Fig. 9) during ACME passage. Foraminifera trapped in the uppermost water layer during ACME passage might have suffered from a high grazing pressure because of the low oxygen eddy core below. The foraminiferal peaks in the deeper trap in April–June 2010 were mostly due to high fluxes of *G. sacculifer* that followed the eddy passage. The increase of foraminiferal flux at both depths in April-June may represent a return to regular (non-eddy) conditions and a recovery/deepening of the thermocline. The actively migrating pteropods (Chang and Yen, 2012) show some decrease in the fluxes in February–March 2010 at both bathypelagic depths (Fig. 7b). This can be explained by the escape from the dead zone area of the approaching eddy and some sedimentation elsewhere.

Missing diel migration of a number of zooplankton groups due to the passage of the suboxic eddy (Karstensen et al., 2015a; Hauss et al., 2015) could have resulted in less organic matter degradation of sinking particles due to reduced “flux feeding”

BGD
12, 18253–18313, 2015

within the suboxic/hypoxic zone (around 40–170 m). This depth range is the most active zone in terms of organic carbon turnover under normal conditions with sufficient oxygen (e.g. Iversen et al., 2010; Hedges, 1992). "Flux feeding" may account for a large part of organic carbon degradation in the uppermost few hundred meters of the water column and determine the shape of the carbon attenuation curve (Iversen et al., 2010), although quantitative estimates are lacking. Under oxic conditions, overall carbon-specific respiration due to microbial degradation is estimated to be 0.13 d^{-1} in the uppermost ocean (Iversen and Ploug, 2010, 2013; Iversen et al., 2010), independent of particle size and type. It is likely that the severe hypoxia/suboxia reduced both oxic microbial respiration and zooplankton "flux feeding". As a result, the organic carbon flux to greater depths might have increased.

6 Summary

The impact of a low oxygen eddy (ACME) on particle fluxes at the CVOO mooring site has been investigated from two sediment traps time series covering the period from December 2009 to May 2011. The eddy passage was recorded in February 2010 with the onset of very low (< 2 µmol L^{-1}) dissolved oxygen concentrations observed at very shallow (about 40 m) depth. The eddy passage across the mooring was characterized by a shallowing of the mixed layer (about 20 m depth, Karstensen et al., 2015a) (Fig. 10). Along the reconstructed propagation path of the eddy, from its formation region off the West African coast to the CVOO site (Fig. 1; Karstensen et al., 2015a), satellite derived chlorophyll maps reveal surface signatures of high chlorophyll standing stocks within the eddy (Fig. 1). The schematic Fig. 10 summarizes the most important processes and the responses in the bathypelagic ocean to the eddy passage:

– BSi, diatoms and organic carbon fluxes increased and seasonality was unusually high in winter–spring 2010 when the ACME passed, compared to 2011 during a non-eddy year,

BGD
12, 18253–18313, 2015

– organic carbon flux increased in February 2010, corresponding perfectly to mineral dust flux, suggesting a close coupling between the input from land and the biological pump,

– diatoms showed no signature from coastal environments but were mostly of pelagic origin, suggesting a pronounced alteration of the eddy since its origin at the African coast in summer 2009,

– molar C : N ratios of organic matter were unusually high (18–25) in February 2010, although nutrient supply is high within the ACMEs (Karstensen et al., 2015b). This may indicate that some production was under nutrient (nitrate) limitation (e.g. Löscher et al., 2015a), probably combined with low growth rates in the beginning of 2010,

– biomarker studies provided no evidence of green sulfur bacteria nor bacteria characteristic for anammox, both of which might be present under suboxic conditions or in OMZs,

– δ^{15}N ratios declined from 5.2 to 3.1 ‰ from January to March 2010 during the approaching and passing ACME, combined with a peak in nitrogen flux in February–March 2010,

– carbonate fluxes decreased in February 2010, mainly due to declining pteropod fluxes and fluxes of near-surface dwelling planktonic foraminifera. Subsurface dwellers such as *G. menardii*, however, showed distinct flux peaks in both traps in February 2010 (Fig. 10), most probably due to the development of low oxygen conditions in the subsurface waters of the ACME,

– coccolithophores as major primary carbonate producers appear to be less affected by the ACME passage. Surface-near *E. huxleyi* and other species showed an increase in fluxes in February 2010, the deeper living *F. produnda* reduced their contribution slightly,

BGD
12, 18253–18313, 2015

– we have no indications of any carbonate dissolution due to a reduced pH (~ 7.6, Fiedler et al., 2015) within the suboxic/hypoxic parts of the ACME through which the particles have to sink,

– sinking detritus and organic matter degradation might have contributed to the severe suboxia/hypoxia in February 2010 in the subsurface waters. We assume that the severe suboxia began in the beginning of 2010,

– sedimentation from the eddy might have occurred due to nutrient exhaustion and/or deposition of mineral dust combined with enhanced chlorophyll in December 2009 and January 2010 (Fig. 10),

– daily migrating zooplankton is reduced in low oxygen eddies (Karstensen et al., 2015a; Hauss et al., 2015) which should have resulted in less organic matter degradation due to missing "flux feeding". This could have resulted in less organic carbon flux attenuation and thus, a higher bathypelagic organic carbon flux.

7 Conclusions and outlook

The passage of the eddy (ACME) with the suboxia in the subsurface waters which was studied at CVOO may serve as a natural experiment or open-ocean "mesocosm" with respect to particle sedimentation. Oceanic oxygen levels in the future oceans might decrease significantly and develop into OMZs due to global warming and increased water column stratification (e.g. Stramma et al., 2008, 2010; Codispoti, 2010; Löscher et al., 2015a). These potential changes might influence the nitrogen cycle and the operation of the biological pump, e.g. via a better preservation of organic materials due to reduced or non-existing microbial respiration (Iversen and Ploug, 2010) combined with reduced zooplankton activities (missing "flux feeding") within the developing OMZs. Such processes could enhance marine CO_2 sequestration and operate as a negative feedback on global warming.

BGD
12, 18253–18313, 2015

The studies are further interesting when considering warm periods in the Earth's history (e.g. the Upper Cretaceous) when OMZs were widely expanded and black shales with high organic carbon contents have been deposited (e.g. Takashima et al., 2006; Schönfeld et al., 2015). This study may contribute to the unsolved question of production versus preservation of organic materials when trying to explain the origin of black shales and oil source rocks in the Earth's history (e.g. Calvert, 1987). In addition, sedimentation signals with erratic character such as peaks in large diatoms in pelagic sediments below oligotrophic areas of the world ocean (e.g. *Ethmodiscus* rex in South Atlantic, Romero and Schmieder, 2006) might be explained by processes occurring within recurring eddies. For instance, the Agulhas current system with its retroflection zone releases continuously large numbers of different types of eddies both into the northwest into the South Atlantic and the Southern Ocean. These eddies may serve as productive oasis within generally oligotrophic ocean deserts and become suboxic/hypoxic at some time, probably depending on the amount and type of organic-rich marine snow particles being remineralized in its subsurface waters (e.g. Löscher et al., 2015b; Karstensen et al., 2015a) as well as on specific eddy physics.

Among others, remaining questions concerning the processes within suboxic/hypoxic eddies are:

1. what are the sedimentation processes associated with these eddies from local and global perspectives? Are such eddies characterized by pulsed sedimentation or a more continuous particle rain? Which processes might trigger pulsed sedimentation events within an eddy?

2. how frequent are these eddies and why do suboxia develop in their subsurface waters?

3. what is the impact of the different groups of zooplankton (tolerating different oxygen levels) on particle flux and export within the eddies but in other OMZs as well?

BGD
12, 18253–18313, 2015

4. how much do different types of eddies contribute (e.g. on an annual/seasonal basis) to export and sedimentation at certain key locations?

Further studies are required for a better knowledge of eddy-induced processes in the surface (production) and subsurface waters (preservation), e.g. the observation and study of eddies when developing to suboxia/hypoxia, the changing N-cycle, combined with measurements including the export into the epipelagic and the upper mesopelagic. The latter could be achieved for instance with free-drifting sediment traps equipped with optical instruments and/or neutrally buoyant sediment traps (e.g. Buesseler et al., 2007). In doing so, we can study organic carbon production versus degradation processes with oxygen minima in more detail.

Author contributions. G. Fischer wrote the ms, together with the co-authors, J. Karstensen designed the mooring, analyzed the current meter data and contributed to writing as well, O. Romero studied the diatoms and contributed to the discussion, K.-H. Baumann studied the coccolithophorides, B. Donner the planktonic foraminifera, J. Hefter and G. Mollenhauer measured and interpreted the lipid biomarkers, M. Iversen investigated the zooplankton, B. Fielder the nitrogen cycle, I. Monteiro did the biogeochemistry at CVOO. A. Körtzinger is coordinating the entire program and contributed to the discussion.

Acknowledgements. We are grateful to G. Niehus and U. Papenburg (GEOMAR) for their help and the deployment of the mooring arrays at CVOO. We would like to thank the crews, masters and chief scientist P. Brandt of *l'Atalante 2008*, MSM *Merian* 18/2 and RV *Meteor* 80/1 (all GEOMAR). At marum, G. Ruhland and M. Klann were responsible for the preparation of the sediment traps and laboratory work. At the ZMT (Leibniz Center of Tropical Marine Ecology, Bremen), Dorothee Dasbach measured the stable nitrogen ratios, thanks also go to Birgit Mayer-Schack (marum) for sample preparation. This work was funded through the DFG-Research Centers/Clusters of Excellence "The Ocean in the Earth System" at the Marum Centre of Marine Environmental Research, Bremen University and "The Future Ocean" at the CAU, Kiel. Additional support was provided by the DFG Collaborate Research Centre 754 (www.sfb754.de). Satellite data was made available from MODIS website (http://oceancolor.gsfc.nasa.gov/). CVOO is part of the OceanSITES network.

BGD
12, 18253–18313, 2015

References

Altabet, M. and Deuser, W. G.: Seasonal variations in natural abundance of 15N in particles sinking to the deep Sargasso Sea, Nature, 315, 218–219, 1985.

Altabet, M., Deuser, W. G., Honjo, S., and Steinen, C.: Seasonal and depth-related changes in the source of sinking particles in the North Atlantic, Nature, 354, 36–139, 1991.

Andruleit, H., Stäger, S. and Rogalle, U.: Living coccolithophores in the northern Arabian Sea: ecological tolerances and environmental control, Mar. Micropaleontol., 49, 157–181, 2003.

Ansmann, A., Petzold, A., Kandler, K., Tegen, I., Wendisch, M., Müller, D., Weinzierl, B., Müller, T., and Heintzenberg, J.: Saharan Mineral dust experiments SAMUM-1 and SAMUM-2: what have we learned?, Tellus B, 63, 403–429, 2011.

Armstrong, R. A., Lee, C., Hedges, J. I., Honjo, S., and Wakeham, S. G.: A new, mechanistic model of organic carbon fluxes in the ocean based on the quantitative association of POC with ballast minerals, Deep-Sea Res. Pt. II, 49, 219–236., 2002.

Ayon, P., Criales-Hernandez, M. I., Schwamborn, R., and Hirche, H.-J.: Zooplankton research off Peru: a review, Prog. Oceanogr., 79, 238–255, 2008.

Barton, E. D., Arístegui, J., Tett, P., Cantón, M., García-Braun, J., Hernández-León, S., Nykjaer, L., Almeida, C., Almunia, J., Ballesteros, S., Basterretxea, G., Escánez, J., García-Weill, L., Hernández-Guerra, A., López-Laatzen, F., Molina, P., Montero, M. F., Navarro-Pérez, E., Rodriguez, J. M., van Lenning, K., Vélez, H., and Wild, K.: Eastern Boundary of the North Atlantic: Northwest Africa and Iberia, in: The Global Coastal Ocean, edited by: Robinson, A. R., and Brink, K., John Wiley and Sons, New York, Chichester, Weinheim, Brisbane, Singapore, Toronto, Vol. 11, 29–67, 1998.

Boeckel, B. and Baumann, K.-H.: Vertical and lateral variations in coccolithophore community structure across the subtropical frontal zone in the South Atlantic Ocean, Mar. Micropaleontol., 67, 255–273, 2008.

Benitez-Nelson, C. R. and McGullicuddy, D. J.: Mesoscale physical-biological-biogeochemical linkages in the open ocean: an introduction to the results of the E-Flux and EDDIES programs, Deep-Sea Res. Pt. I, 55, 1133–1138, 2008.

Berelson, W. M.: Particle settling rates increase with depth in the ocean, Deep-Sea Res. Pt. II, 49, 237–251, 2002.

Berger, W. H. and Wefer, G.: Export production: seasonality and intermittency, and paleoceanographic implications, Palaeogeogr. Palaeoecol., 89, 245–254, 1990.

BGD
12, 18253–18313, 2015

Bory, A., Jeandel, C., Leblond, N., Vangriesheim, A., Khripounoff, A., Beaufort, L., Rabouille, C., Nicolas, E., Tachikawa, K., Etcheber, H., and Buat-Menard, P.: Particle flux within different productivity regimes off the Mauritanian upwelling zone (EUMELI program), Deep-Sea Res. Pt. II, 48, 2251–2282, 2001.

Boyd, P. W. and Trull, T. W.: Understanding the export of biogenic particles in oceanic waters: is there a consensus?, Prog. Oceanogr., 72, 276–312, 2007.

Buesseler, K. O., Antia, A. A., Chen, M., Fowler, S. W., Gardner, W. D., Gustafsson, O., Harada, K., Michaels, A. F., Rutgers van der Loeff, M., Sarin, M., Steinberg, D. K., and Trull, T.: An assessment of the use of sediment traps for estimating upper ocean particle fluxes, J. Mar. Res., 65, 345–416, 2007.

Calvert, S. E.: Oceanographic controls on the accumulation of organic matter in marine sediments, Geol. Soc. S. P., 26, 137–151, doi:10.1144/GSL.SP.1987.026.01.08, 1987.

Chang, Y., and Yen, J.: Swimming in the intermediate reynolds range: kinematics of the Pteropod *Limacina helicina*, Integr. Comp. Biol., 52, 597–615, doi:10.1093/icb/ics113, 2012.

Chelton, D. B., Gaube, P., Schlax, M. G., Early, J. J., and Samelson, R. M.: The influence of nonlinear mesoscale eddies on near-surface chlorophyll, Science, 334, 328–332, doi:10.1126/science.1208897, 2011.

Codispoti, L. A.: Interesting times for marine N_2O, Science, 327, 1339–1340, doi:10.1126/science.1184945, 2010.

Conte, M. H., Sicre, M.-A., Rühlemann, C., Weber, J. C., Schulte, S., Schulz-Bull, D., and Blanz, T.: Global temperature calibration of the alkenone unsaturation index ($U^{k'}_{37}$) in surface waters and comparison with surface sediments, Geochem. Geophy. Geosy., 7, Q02005, doi:10.1029/2005GC001054, 2006.

Cropper, T. E., Hanna, E., and Bigg, G. R.: Spatial and temporal seasonal trends in coastal upwelling off Northwest Africa, 1981–2012, Deep-Sea Res. Pt. II, 86, 94–111, 2014.

Eltgroth, M. L., Watwood, R. L., and Wolfe, G. V.: Production and cellular localization of neutral long-chain lipids in the haptophyte algae *Isochrysis galbana* and *Emiliania huxleyi*, J. Phycol., 41, 1000–1009, 2005.

Ewart, C. S., Meyers, M. K., Wallner, E. R., McGillicuddy, Jr., D. J., and Carlson, C. A.: Microéial dynamics in cyclonic and anticyclonic mode-water eddies in the Northwestern Sargasso Sea, Deep-Sea Res. Pt. II, 55, 1334–1347, 2008.

BGD
12, 18253–18313, 2015

Fiedler, B., Karstensen, J., Hauss, H., Schütte, F., Grundle, D., Krahmann, G., Santos, C., and Körtzinger, A.: Biogeochemistry of oxygen depleted mesoscale eddies in the open eastern tropical North Atlantic, Biogeosciences Discuss., 2015.

Fischer, G. and Karakas, G.: Sinking rates and ballast composition of particles in the Atlantic Ocean: implications for the organic carbon fluxes to the deep ocean, Biogeosciences, 6, 85–102, doi:10.5194/bg-6-85-2009, 2009.

Fischer, G. and Wefer, G.: Sampling, preparation and analysis of marine particulate matter, in: Marine Particles: Analysis and Characterization, edited by: Hurd, D.C and Spencer, D. W., AGU Monograph Series, 63, Washington, DC, 391–397, 1991.

Fischer, G., Wefer, G., Romero, O., Dittert, N., Ratmeyer, V., and Donner, B.: Transfer of particles into the deep Atlantic and the global Ocean: control of nutrient supply and ballast production, in: The South Atlantic in the Late Quaternary: Reconstruction of Material Budget and Current Systems, edited by: Wefer, G., Mulitza, S., and Ratmeyer, V., Springer, Berlin, Heidelberg, New York, 21–46, 2003.

Fischer, G., Karakas, G., Blaas, M. Ratmeyer, V., Nowald, N., Schlitzer, R., Helmke, P., Davenport, R., Donner, B., Neuer, S., and Wefer, G.: Mineral ballast and particle settling rates in the coastal upwelling system off NW Africa and the South Atlantic, Int. J. Earth Sci., 98, 281–298, doi:10.1007/s00531-007-0234-7, 2009a.

Fischer, G., Reuter, C., Karakas, G., Nowald, N., and Wefer, G.: Offshore advection of particles within the Cape Blanc filament, Mauritania: results from observational and modelling studies, Prog. Oceanogr., 83, 322–330, 2009b.

Fischer, G., Neuer, S., Davenport, R., Romero, O., Ratmeyer, V., Donner, B., Freudenthal, T., Meggers, H., and Wefer, G.: The Northwest African Margin, in: Carbon and Nutrient Fluxes in Continental Margins: a Global Synthesis, edited by: Liu, K. K., Atkinson, L., Quinones, R., and Talaue-McManaus, L., IGBP Book Series, Springer, Berlin, 77–103, 2010.

Fomba, K. W., Müller, K., van Pinxteren, D., Poulain, L., van Pinxteren, M., and Herrmann, H.: Long-term chemical characterization of tropical and marine aerosols at the Cape Verde Atmospheric Observatory (CVAO) from 2007 to 2011, Atmos. Chem. Phys., 14, 8883–8904, doi:10.5194/acp-14-8883-2014, 2014.

Fréon, P., Arístegui, J., Bertrand, A., Crawford, R. J. M., Field, J. C., Gibbons, M. J., Tam, J., Hutchings, L., Masski, H., Mullon, C., Ramdani, M., Seret, B., and Simier, M.: Functional group biodiversity in Eastern Boundary Upwelling Ecosystems questions the wasp-waist trophic structure, Prog. Oceanogr., 83, 97–106, 2009.

BGD
12, 18253–18313, 2015

Gama, C., Tchepel, O., Baldasano, J. M., Basart, S., Ferreira, J., Pio, C., Cardoso, J., and Borrego, C.: Seasonal patterns of Saharan dust over the Cape Verde – a combined approach using observations and modelling, Tellus B, 67, 24410, doi:10.3402/tellusb.v67.24410, 2015.
Goudie, A. S. and Middleton, N. J.: Saharan dust storms: nature and consequences, Earth Sci. Rev., 56, 179–204, 2001.
Hagino, K. and Okada, H.: Intra- and infra-specific morphological variation in selected coccolithophore species in the equatorial and subequatorial Pacific Ocean, Mar. Micropaleontol., 58, 184–206, 2006.
Hagino, K., Okada, H., and Matsuoka, H.: Spatial dynamics of coccolithophore assemblages in the equatorial western-central Pacific Ocean, Mar. Micropaleontol., 39, 53–57, 2000.
Haidar, A. T. and Thierstein, H. R.: Coccolithophore dynamics off Bermuda (N. Atlantic), Deep-Sea Res. Pt. II, 48, 1925–1956, 2001.
Hauss, H., Christiansen, S., Schütte, F., Kiko, R., Edvam Lima, M., Rodrigues, E., Karstensen, J., Löscher, C., Körtzinger, A., and Fiedler, B.: Oasis or dead zone in the open ocean? Zooplankton distribution and migration in low-oxygen modewater eddies, Biogeosciences Discuss., 2015.
Hedges, J. I.: Global biogeochemical cycles: progress and problems, Mar. Chem., 39, 67–93, 1992.
Helmke, P., Romero, O., and Fischer, G.: Northwest African upwelling and its effect on off-shore organic carbon export to the deep sea, Global Biogeochem. Cy., 19, GB4015, doi:10.1029/2004GB002265, 2005.
Hemleben, C., Spindler, M., and Anderson, O. R.: Modern Planktonic Foraminifera, Springer Verlag, Heidelberg, New York, 363 p., 1989.
Holmes, E. M., Lavik, G., Fischer, G. Segl, M., Ruhland, G., and Wefer, G.: Seasonal variability of δ^{15}N in sinking particles in the Benguela upwelling region, Deep-Sea Res. Pt. I, 49, 377–394, 2002.
Honjo, S. and Okada, H.: Community structure of coccolithophores in the photic layer of the mid-Pacific, Micropaleontology, 29, 209–230, 1974.
Honjo, S., Manganini, S. J., Krishfield, R. A., and Francois, R.: Particulate organic carbon fluxes to the ocean interior and factors controlling the biological pump. A synthesis of global sediment trap programs since 1983, Prog. Oceanogr., 76, 217–285, 2008.
Ittekkot, V.: The abiotically driven biological pump in the ocean and short-term fluctuations in atmospheric CO_2 contents, Global Planet. Change, 8, 17–25, 1993.

BGD
12, 18253–18313, 2015

Iversen, M. H. and Ploug, H.: Ballast minerals and the sinking carbon flux in the ocean: carbon-specific respiration rates and sinking velocity of marine snow aggregates, Biogeosciences, 7, 2613–2624, doi:10.5194/bg-7-2613-2010, 2010.

Iversen, M. H. and Ploug, H.: Temperature effects on carbon-specific respiration rate and sinking velocity of diatom aggregates – potential implications for deep ocean export processes, Biogeosciences, 10, 4073–4085, doi:10.5194/bg-10-4073-2013, 2013.

Iversen, M. H. and Robert, M. L.: Ballasting effects of smectite on aggregate formation and export from a natural plankton community, Mar. Chem., 175, 18–27, 2015.

Iversen, M. H., Nowald, N., Ploug, H., Jackson, G. A., and Fischer, G.: High resolution profiles of vertical particulate organic matter export off Cape Blanc, Mauritania: degradation processes and ballasting effects, Deep-Sea Res. Pt. I, 57, 771–784, 2010.

Jickells, T. D., Dorling, S., Deuser, W. G., Church, T. M., Armoto, R., amd Prospero, J. M.: Airborne dust fluxes to a deep water sediment trap in the Sargasso Sea, Global Biogeochem. Cy., 12, 311–320, 1998.

Jickells, T. D., An, Z. N., Andersen, K. K., Baker, A. R., Bergametti, G., Brooks, N., Cao, J. J., Boyd, P. W., Duce, R. A., Hunter, K. A., Kawahata, H., Kubilay, N., la Roche, J., Liss, P. S., Mahowald, N., Prospero, J. M., Ridgwell, A. J., Tegen, I., and Torres, R.: Global iron connections between desert dust, ocean biogeochemistry, and climate, Science, 308, 67–71, 2005.

Jordan, R. W. and Chamberlain, A. H. L.: Biodiversity among haptophyte algae, Biodivers. Conserv., 6, 131–152, 1997.

Karl, D., Christian, J. R., Dore, J. E., Hebel, D. V., Letelier, R. M., Tupas, L. M., Winn, C. D.: Seasonal and interannual variability in primary production and particle flux at Station Aloha, Deep-Sea Res. Pt. II, 43, 539–568, 1996.

Karl, D. M., Bates, N., Harrison, P. J., Jeandel, C., Llinás, O., Liu, K. K., Marty, J.-C., Michaels, A. F., Miquel, J. C., Neuer, S., Nojiri, Y., Wong, C. S.: Temporal studies of biogeochemical processes determined from ocean time-series observations during the JGOFS era, in: Ocean Biogeochemistry: The role of Ocean Carbon Cycle in Global Change, edited by: Fasham, M. J. R., Springer, Berlin, Heidelberg, 239–267, 2003.

Karstensen, J., Fiedler, B., Schütte, F., Brandt, P., Körtzinger, A., Fischer, G., Zantopp, R., Hahn, J., Visbeck, M., and Wallace, D.: Open ocean dead zones in the tropical North Atlantic Ocean, Biogeosciences, 12, 2597–2605, doi:10.5194/bg-12-2597-2015, 2015a.

BGD
12, 18253–18313, 2015

Karstensen, J., Schütte, F., Pietri, A., Krahmann, G., Fiedler, B., Grundle, D., Hauss, H., Körtzinger, A., Löscher, C., and Viera, N.: Anatomy of open ocean dead-zones based on high-resolution multidisciplinary glider data, Biogeosciences Discuss., 2015b.

Kaufman, Y. J., Koren, I., Remer, L. A., Tanre', D., Ginoux, P., and Fan, S.: Dust transport and deposition from the Terra-Moderate Resolution Imaging Spectroradiometer (MODIS) spacecraft over the Atlantic Ocean, J. Geophys. Res., 110, D10S12, doi:10.1029/2003JD004436, 2005.

Koopmans, M. P., Koster, J., Van Kaam-Peters, H. M. E., Kenig, F., Schouten, S., Hartgers, W. M., De Leeuw, J. W., Sinninghe Damsté, J. S.: Diagenetic and catagenetic products of isorenieratene: molecular indicators for photic zone anoxia, Geochim. Cosmochim. Ac., 60, 4467–4496, 1996.

Kremling, K., Lentz, U., Zeitzschell, B., Schulz-Bull, D. E., and Duinker, J. C.: New type of time-series sediment trap for the reliable collection of inorganic and organic trace chemical substances, Rev. Sci. Instrum., 67, 4360–4363, 1996.

Kucera, M.: Planktonic foraminifera as tracers of past oceanic environments, in: Proxies in Late Cenozoic Paleoceanography: Developments in Marine Geology, edited by: Hillaire-Marcel, C. and de Verna, A., Elsevier, Amsterdam, Vol. 1, 213–262, 2007.

Lampitt, R. S. and Antia, A. N.: Particle flux in deep seas: regional characteristics and temporal variability, Deep-Sea Res. I, 44, 1377–1403, 1997.

Laws, E. E. and Bannister, T. T.: Nutrient- and light-limited growth of *Thalassiosira fluviatilis* in continuous culture, with implications for phytoplankton growth in the ocean, Limnol. Oceanogr., 25, 457–473, 1980.

Libes, S. M. and Deuser, W. G.: The isotopic geochemistry of particulate nitrogen in the Peru Upwelling Area and the Gulf of Maine, Deep-Sea Res. I, 35, 517–533, 1988.

Liu, K. K. and Kaplan, I. R.: The eastern tropical Pacific as a source of ^{15}N-enriched nitrate in seawater off southern California, Limnol. Oceanogr., 34, 820–830, 1989.

Loebl, M., Cockshutt, A. M., Campbell, D. A., and Finkel, Z. V.: Physiological basis for high resistance to photoinhibition under nitrogen depletion in *Emiliania huxleyi*, Limnol. Oceanogr., 55, 2150–2160, doi:10.4319/lo.2010.55.5.2150, 2010.

Löscher, C. R., Bange, H. W., Schmitz, R. A., Callbeck, C. M., Engel, A., Hauss, H., Kanzow, T., Kiko, R., Lavik, G., Loginova, A., Melzner, F., Neulinger, S. C., Pahlow, M., Riebesell, U., Schunck, H., Thomson, S., and Wagner, H.: Water column biogeochemistry of oxygen minimum zones in the eastern tropical North Atlantic and eastern tropical South Pacific Oceans,

BGD
12, 18253–18313, 2015

Biogeosciences Discuss., 12, 4495–4556, 2015a, http://www.biogeosciences-discuss.net/12/4495/2015/.
Löscher, C. R., Fischer, M. A., Neulinger, S. C., Fiedler, B., Philippi, M., Schütte, F., Singh, A., Hauss, H., Karstensen, J., Körtzinger„ A., Künzel, S., and Schmitz, R. A.:. Hidden biosphere in an oxygen-deficient Atlantic open ocean eddy: future implications of ocean deoxygenation on primary production in the eastern tropical North Atlantic, Biogeosciences Discuss., 12, 14175–14213, doi:10.5194/bgd-12-14175-2015, 2015b.
Luyten, J. R., Pedlowski, J., and Stommel, H.: The ventilated thermocline, J. Phys. Oceanogr., 13, 292–309, 1983.
Malinverno, E., Ziveri, P., and Corselli, C.: Coccolithophorid distribution in the Ionian Sea and its relationship to eastern Mediterranean circulation during late fall to early winter 1997, J. Geophys. Res., 108, 8115, doi:10.1029/2002JC001346, 2003.
Mariotti, A., Mariotti, F., Champigny, M.-L., Amarger, N., and Moyse, A.: Nitrogen isotope fractionation associated with nitrate reductase activity and uptake of NO_3 by pearl millet, Plant Physiol., 69, 880–884, 1982.
Martiny, A. C., Pham, C. T. A., Primeau, F. W., Vrugt, J. A., Moore, J. K., Levin, S. A., and Lomas, M. W.: Strong latitudinal patterns in the elemental ratios of marine plankton and organic matter, Nat. Geosci., 6, 279–283, 2013.
McGillicuddy, D. J., Anderson, L. A., Bates, N. R., Bibby, T., Buesseler, K. O., Carlson, C. A., Davis, C. S., Ewart, C., Falkowski, P. G., Goldthwait, S. A., Hansell, D. A., Jenkins, W. J., Johnson, R., Kosnyrev, V. K., Ledwell, J. R., Li, Q. P., Siegel, D. A., and Steinberg, D. K.: Eddy/wind interactions stimulate extraordinary mid-ocean plankton blooms, Science, 316, 1021–1026, doi:10.1126/science.1136256, 2007.
McNeil, J. D., Jannasch, H. W., Dickey, T., McGillicuddy, D., Brzezinski, M., and Sakamoto, C. M.: New chemical, bio-optical and physical observations of upper ocean response to the passage of a mesoscale eddy off Bermuda, J. Geophys. Res.-Oceans, 104, 15537–15548, 1999.
Müller, P. J.: C/N ratios in Pacific deep-sea sediments: effects of inorganic ammonium and organic nitrogen compounds sorbed by clays, Geochim. Cosmochim. Ac., 41, 765–776, 1977.
Müller, P. J. and Schneider, R. An automated leaching method for the determination of opal in sediments and particulate matter, Deep-Sea Res. Pt. I, 40, 425–444, 1993.
Moulin, C., Lambert, C. E., Dulac, F., and Dayan, U.: Control of atmospheric export of dust from North Africa by the North Atlantic Oscillation, Nature, 387, 691–694, 1997.

BGD
12, 18253–18313, 2015

Neuer, S., Davenport, R., Freudenthal, T., Wefer, G., Lineás, O., Rueda, M.-J., Steinberg, D., and Karl, D.: Differences in the biological carbon pump at three subtropical ocean sites, Geophys. Res. Lett., 29, 1885, doi:10.1029/2002GL015393, 2002.

Neuer, S., Cianca, A., Helmke, P., Freudenthal, T., Davenport, R., Meggers, H., Knoll, M., Santana-Casiano, J. M., González-Davila, M., Rueda, M.-J., and Llinás, O.: Biogeochemistry and hydrography in the eastern subtropical North Atlantic gyre. Results from the European time-series station ESTOC, Prog. Oceanogr., 72, 1–29, 2007.

Okada, H. and Honjo, S.: The distribution of oceanic coccolithophorids in the Pacific, Deep-Sea Res. Pt. I, 20, 355–374, 1973.

Ploug, H., Iversen, M. H., and Fischer, G.: Ballast, sinking velocity, and apparent diffusivity within marine snow and fecal pellets: implications for substrate turnover by attached bacteria, Limnol. Oceanogr., 53, 1878–1886, 2008.

Prahl, F. G. and Wakeham, S. G.: Calibration of unsaturation patterns in long-chain ketone compositions for palaeotemperature assessment, Nature, 330, 367–369, 1987.

Prahl, F. G., Wolfe, G. V., and Sparrow, M. A.: Physiological impacts on alkenone paleothermometry, Paleoceanography, 18, 1025, doi:10.1029/2002PA000803, 2003.

Ragueneau, O., Treguer, P., Leynaert, A., Anderson, R. F., Brzezinski, M. A., DeMaster, D. J., Dugdale, R. C., Dymond, J., Fischer, G., Francois, R., Heinze, C., Maier-Reimer, E., Martin-Jezequel, V., Nelson, D. M., and Queguiner, B.: A review of the Si cycle in the modern ocean: recent progress and missing gaps in the application of biogenic opal as a paleoproductivity proxy, Global Planet. Change, 26, 317–365, 2000.

Ratmeyer, V., Balzer, W., Bergametti, G., Chiapello, I., Fischer, G., and Wyputta, U.: Seasonal impact of mineral dust on deep-ocean particle flux in the eastern subtropical Atlantic Ocean, Mar. Geol., 159, 241–252, 1999.

Redfield, A. C., Ketchum, B. H., and Richards, F. A.: The influence of organisms on the composition of seawater, in: The Sea, edited by Hill, M. N., Vol. 2, Wiley and Sons, Chichester, 26–77, 1963.

Romankevich, E. A.: Geochemistry of OM in the Ocean, Springer, Berlin, Heidelberg, New York, 334 p., 1984.

Romero, O. E. and Armand, L. K.: Marine diatoms as indicators of modern changes in oceanographic conditions, in: The Diatoms, Applications for the Environmental and Earth Sciences, 2nd edn., eidted by: Smol, J. P. and Stoermer, E. F., Cambridge University Press, Cambridge, 373–400, 2010.

BGD
12, 18253–18313, 2015

Romero, O. E. and Schmieder. F.: Occurrence of thick *Ethmodiscus* oozes associated with a terminal Mid-Pleistocene Transition event in the oligotrophic subtropical South Atlantic, Palaeogeogr. Palaeoecol., 235, 321–329, 2006.
Romero, O. E., Lange, C. B., and Wefer, G.: Interannual variability (1988–1991) of siliceous phytoplankton fluxes off northwest Africa, J. Plankton Res., 24, 1035–1046, 2002.
Romero, O., Crosta, E. X., Kim, J.-H., Pichevin, L., and Crespin, J.: Rapid longitudinal migrations of the filament front off Namibia (SE Atlantic) during the past 70 kyr, Global Planet. Change, 125, 1–12, 2015.
Round, F. E., Crawford, R. M., and Mann, D. G.: The Diatoms, Cambridge University Press, Cambridge, 747p., 1990.
Ryabenko, E., Kock, A., Bange, H. W., Altabet, M. A., and Wallace, D. W. R.: Contrasting biogeochemistry of nitrogen in the Atlantic and Pacific Oxygen Minimum Zones, Biogeosciences, 9, 203–215, doi:10.5194/bg-9-203-2012, 2012.
Saino, T. and Hattori, A.: Geographical variation of the water column distribution of suspended particulate organic nitrogen and its 15N natural abundance in the Pacific and its marginal seas, Deep-Sea Res. Pt. I, 34, 807–827, 1987.
Sancetta, C. and Calvert, S. E.: The annual cycle of sedimentation in Saanich Inlet, British Columbia: implications for the interpretation of diatom fossil assemblages, Deep-Sea Res. Pt. I., 35, 71–90, 1988.
Schäfer, P. and Ittekkot, V.: Seasonal variability in δ^{15}N in settling particles in the Arabian Sea and its paleogeochemical significance, Naturwissenschaften, 80, 511–513, 1983.
Schepanski, K., Tegen, I., and Macke, A.: Saharan dust transport and deposition towards the tropical northern Atlantic, Atmos. Chem. Phys., 9, 1173–1189, doi:10.5194/acp-9-1173-2009, 2009.
Schönfeld, J., Kuhnt, W., Erdem, Z., Flögel, S., Glock, N., Aquit, M., Frank, M., and Holbourn, A.: Records of past mid-depth ventilation: cretaceous ocean anoxic event 2 vs. recent oxygen minimum zones, Biogeosciences, 12, 1169–1189, doi:10.5194/bg-12-1169-2015, 2015.
Schrader, H.-J. and Gersonde. R.: Diatoms and silicoflagellates. Utrecht micropaleontological bulletin, in: Micropaleontological Counting Methods and Techniques – an Exercise on an Eight Meter Section of the Lower Pliocene of Capo Rosello, Sicily, edited by: Zachariasse, W. J., Riedel, W. R., Sanfilippo, A., Schmidt, R. R., Brolsma, M. J., Schrader, H., Gersonde, R., Drooger, M. M., and Broekman, J. A., C. W. Drooger, Utrecht, 17, 129–176, 1978.

BGD
12, 18253–18313, 2015

Schütte, F., Brandt, P., and Karstensen, J.: Occurrence and characteristics of mesoscale eddies in the tropical northeast Atlantic Ocean, Ocean Sci., 2015a.
Schütte, F., Karstensen, J., Krahmann, G., Fiedler, B., Brandt, P., Visbeck, M., and Körtzinger, A.: Characterization of "dead-zone eddies" in the tropical North Atlantic Ocean, Biogeosciences Discuss., 2015b.
Schütz, L., Jaenicke, R., and Pietreck, H.: Saharan dust transport over the North Atlantic Ocean: model calculations and measurements. in: Desert Dust, edited by: Péwé, T. L., Geol. Soc. Amer. Spec. Publ., 186, 87–100, 1981.
Siegel, D. A. and Deuser, W. G.: Trajectories of sinking particles in the Sargasso Sea: modeling of statistical funnels above deep-ocean sediment traps, Deep-Sea Res. Pt. I, 44, 1519–1541, 1997.
Sikes, E. L., O'Leary, T., Nodder, S. D., and Volkman, J. K.: Alkenone temperature records and biomarker flux at the subtropical front on the chatham rise, SW Pacific Ocean, Deep-Sea Res. Pt. I, 52, 721–748, doi:10.1016/j.dsr.2004.12.003, 2005.
Sinninghe Damste, J. S., Strous, M., Rijpstra, W. I. C., Hopmans, E. C., Geenevasen, J. A. J., Van Duin, A. C. D., Van Niftrik, L. A., and Jettenk, M. S. M.: Linearly concatenated cyclobutane lipids form a dense bacterial membrane, Nature, 419, 708–712, 2002.
Stramma, L., Johnson, G. C., Sprintall, J., and Mohrholz, V.: Expanding oxygen-minimum zones in the tropical oceans, Science, 320, 655–658, 2008.
Stramma, L., Schmidtko, S., Levin, L. A., and Johnson, G. C.: Ocean oxygen minima expansions and their biological impacts, Deep-Sea Res. Pt. I, 57, 587–595, doi:10.1016/j.dsr.2010.01.005, 2010.
Sweeney, E. N., McGillicuddy, D. J., and Buesseler, K. O.: Biogeochemical impacts due to mesoscale eddy activity in the Sargasso Sea as measured at the Bermuda Atlantic Time Series Study (BATS), Deep-Sea Res. Pt. II, 50, 3017–3039, 2003.
Takahashi, K. and Okada, H.: Environmental control on the biogeography of modern coccolithophores in the southeastern Indian Ocean offshore of Western Australia, Mar. Micropaleontol., 39, 73–86, 2000.
Takashima, R., Hishi, H., Huber, B., and Leckie, M.: Greenhouse world and the Mesozoic ocean, Oceanography, 19, 82–92, 2006.
Tyson, R. V.: Sedimentary OM: organic facies and palynofacies, Chapman and Hall, London, 615 p., 1995.

BGD
12, 18253–18313, 2015

Van Camp, L., Nykjaer, L., Mittelstaedt, E., and Schlittenhardt, P.: Upwelling and boundary circulation off Northwest Africa as depicted by infrared and visible satellite observations, Prog. Oceanogr., 26, 357–402, 1991.

Wagner, T. and Dupont, L. M.: Terrestrial organic matter in marine sediments: analytical approaches and eolian-marine records in the Central Equatorial Atlantic, in: Use of Proxies in Paleoceanography: Examples from the South Atlantic, edited by: Fischer, G. and Wefer, G., Springer, Berlin, Heidelberg, 547–574, 1999.

Yu, E. F., Francois R., Honjo, S., Fleer, A. P., Manganini, S. J., Rutgers van der Loeff, M. M., and Ittekkot, V.: Trapping efficiency of bottom-tethered sediment traps estimated from the intercepted fluxes of ^{230}Th and ^{231}Pa, Deep-Sea Res. Pt. I, 48, 865–889, 2001.

Zenk, W., Klein, B., and Schroder, M.: Cape verde frontal zone, Deep-Sea Res. Pt. I, 38, 505–530, 1991.

BGD
12, 18253–18313, 2015

Table 1. Collection dates for the upper (1290 m) and lower (3439 m) traps, bulk mass fluxes and composition, molar C : N ratios of organic matter and δ^{15}N (only lower trap).

CVOO-3 upper sample #	cup cpened	cup closed	duration days	Mass fluxes in mg m^{-2} d^{-1} total mass	biogenic opal	organic carbon	nitrogen	carbonate	lithogenic	Composition in % biogenic opal	organic carbon	nitrogen	carbonate	lithogenic	ratio C/N molar
1	01.12.09	30.12.09	29	51.24	2.01	2.81	0.34	29.56	14.05	3.92	5.48	0.66	57.69	27.42	9.8
2	30.12.09	28.01.10	29	36.18	0.46	1.69	0.18	28.90	3.43	1.28	4.68	0.50	79.88	9.48	10.8
3	28.01.10	26.02.10	29	68.66	3.11	6.18	0.40	21.23	31.96	4.53	9.00	0.59	30.92	46.55	17.8
4	26.02.10	27.03.10	29	45.76	3.57	2.58	0.29	33.50	3.54	7.80	5.63	0.63	73.20	7.73	10.4
5	27.03.10	25.04.10	29	49.58	0.99	3.67	0.46	35.54	5.72	1.99	7.41	0.93	71.67	11.53	9.3
6	25.04.10	24.05.10	29	33.17	0.89	1.77	0.28	30.64	0.00	2.67	5.34	0.84	92.36	0.00	7.4
7	24.05.10	22.06.10	29	53.27	0.85	4.10	0.39	42.27	1.95	1.60	7.69	0.72	79.35	3.66	12.4
8	22.06.10	21.07.10	29	27.95	0.44	1.76	0.18	22.51	1.48	1.57	6.29	0.66	80.53	5.31	11.2
9	21.07.10	19.08.10	29	14.93	0.40	0.78	0.14	13.10	0.00	2.69	5.21	0.95	87.75	0.00	6.4
10	19.08.10	17.09.10	29	14.25	0.20	1.16	0.19	10.18	1.55	1.39	8.16	1.30	71.42	10.88	7.3
11	17.09.10	16.10.10	29	17.63	0.05	1.47	0.20	10.19	4.45	0.29	8.34	1.12	57.79	25.24	8.7
12	16.10.10	14.11.10	29	9.83	0.09	0.80	0.06	4.93	3.21	0.93	8.13	0.63	50.17	32.64	15.0
13	14.11.10	13.12.10	29	6.88	0.15	0.73	0.08	3.23	2.03	2.17	10.64	1.16	46.98	29.57	10.7
14	13.12.10	11.01.11	29	9.03	0.11	0.49	0.05	7.21	0.73	1.17	5.44	0.55	79.86	8.08	11.5
15	11.01.11	09.02.11	29	19.06	0.17	1.28	0.16	15.94	0.39	0.91	6.70	0.83	83.62	2.07	9.4
16	09.02.11	10.03.11	29	18.83	0.22	1.29	0.15	15.35	0.68	1.18	6.84	0.79	81.53	3.60	10.1
17	10.03.11	08.04.11	29	17.53	0.74	1.49	0.17	10.83	2.98	4.24	8.49	0.97	61.77	17.02	10.2
18	08.04.11	07.05.11	29	10.34	0.34	0.71	0.10	8.93	0.00	3.25	6.89	1.00	86.37	0.00	8.1
g m^{-2}/522 days		**522**		**15.26**	**0.43**	**1.01**	**0.11**	**9.98**	**2.27**	**2.81**	**6.61**	**0.73**	**65.38**	**14.85**	**10.6**

BGD
12, 18253–18313, 2015

Table 1. Continued.

CVOO-3 lower sample #	cup opened	cup closed	duration days	Mass fluxes in mg m^{-2} d^{-1} total mass	biogenic opal	organic carbon	nitrogen	carbonate	lithogenic	Composition in % biogenic opal	organic carbon	nitrogen	carbonate	lithogenic	ratio C/N molar	$\delta^{15}N$ ‰
1	01.12.09	30.12.09	29	124.97	4.40	5.32	0.57	62.56	47.36	3.52	.26	0.46	50.06	37.90	10.9	4.24
2	30.12.09	28.01.10	29	94.75	3.10	3.41	0.37	51.97	32.86	3.27	3.60	0.39	54.85	34.69	10.8	5.21
3	28.01.10	26.02.10	29	151.05	12.58	13.31	0.63	21.40	90.45	8.33	8.81	0.42	14.17	59.88	24.5	3.81
4	26.02.10	27.03.10	29	121.93	14.94	4.63	0.63	61.04	36.69	12.25	3.80	0.52	50.06	30.09	8.6	3.11
5	27.03.10	25.04.10	29	76.17	3.34	4.60	0.42	35.29	28.34	4.39	6.04	0.56	46.33	37.20	12.7	3.21
6	25.04.10	24.05.10	29	56.24	2.82	.95	0.37	31.99	15.52	5.01	5.25	0.66	56.89	27.60	9.3	3.93
7	24.05.10	22.06.10	29	26.33	0.51	1.19	0.13	19.33	4.11	1.93	4.53	0.49	73.42	15.60	10.8	3.5
8	22.06.10	21.07.10	29	19.12	0.43	0.88	0.11	13.77	3.15	2.25	4.61	0.58	72.03	16.49	9.4	3.18
9	21.07.10	19.08.10	29	13.39	0.34	0.79	0.09	8.23	3.25	2.53	5.89	0.67	61.44	24.24	10.3	5.35
10	19.08.10	17.09.10	29	22.38	0.68	1.42	0.15	11.30	7.57	3.04	6.33	0.67	50.50	33.81	11.1	3.32
11	17.09.10	16.10.10	29	9.28	0.24	0.56	0.06	5.23	2.70	2.61	6.01	0.60	56.29	29.07	11.7	4.22
12	16.10.10	14.11.10	29	17.68	0.39	1.01	0.08	10.10	5.17	2.20	5.73	0.47	57.12	29.22	14.3	3.47
13	14.11.10	13.12.10	29	19.14	0.68	1.23	0.16	10.20	5.81	3.54	6.40	0.84	53.30	30.36	8.9	6.99
14	13.12.10	11.01.11	29	7.16	0.20	0.37	0.04	4.19	2.02	2.73	5.22	0.58	58.60	28.24	10.5	4.82
15	11.01.11	09.02.11	29	10.50	0.11	0.64	0.08	7.35	1.75	1.02	6.13	0.73	70.01	16.72	9.8	4.16
16	09.02.11	10.03.11	29	6.78	0.11	0.34	0.04	5.68	0.30	1.57	5.09	0.52	3.84	4.42	11.4	3.42
17–19	10.03.11	11.05.11	62.6	4.12	0.16	0.36	0.04	2.32	0.93	3.84	8.66	0.91	56.28	22.55	11.1	4.79
g m^{-2}/527 days				**526.6**												

BGD
12, 18253–18313, 2015

Table 2. Fluxes of major primary and secondary producers/organisms (diatoms, diatom coastal : pelagic ratio, coccolithophores and planktonic foraminifera) for the upper trap samples.

CVOO-3 upper sample #	cup opened	cup closed	duration days	Diatom flux valves $m^{-2} d^{-1}$	coastal : pelagic ratio of diatoms	Coccolith flux no. $*10^6 m^{-2} d^{-1}$	*E. huxleyi*	*F. profunda*	Foram. flux ind. $m^{-2} d^{-1}$	*G. ruber* w + p	*G. sacculifer*	*G. menardii*	Foram. mass flux mg carbonate $m^{-2} d^{-1}$	Pteropod mass flux mg carbonate $m^{-2} d^{-1}$
1	01.12.09	30.12.09	29	104 104	0.16	938	171	296		129	38	31	6.3	2.5
2	30.12.09	28.01.10	29	36 139	0.04	667	89	213		147	117	23	10.5	2.2
3	28.01.10	26.02.10	29	97 753	0.08	1298	305	420		33	40	164	11.1	0.9
4	26.02.10	27.03.10	29	117 544	0.07	612	112	184		115	204	80	10.6	1.2
5	27.03.10	25.04.10	29	171 167	0.09	952	155	418		108	131	0	14.8	3.5
6	25.04.10	24.05.10	29	38 330	0.08	819	121	343		77	105	33	11.4	3.6
7	24.05.10	22.06.10	29	55 195	0.09	731	100	360		90	244	93	21.5	1.3
8	22.06.10	21.07.10	29	22 341	0.14	793	120	358		57	42	31	5.1	1.3
9	21.07.10	19.08.10	29	13 142	0.03	431	84	155		14	8	7	0.9	4.2
10	19.08.10	17.09.10	29	16 865	0.04	403	47	130		34	20	20	2.5	2.0
11	17.09.10	16.10.10	29	6388	0.07	182	19	87		34	22	32	3.5	3.7
12	16.10.10	14.11.10	29	n.d.	n.d.	190	24	93		13	11	8	2.1	1.9
13	14.11.10	13.12.10	29	2300	0.00	77	16	29		3	3	2	0.4	0.8
14	13.12.10	11.01.11	29	n.d.	n.d.	178	26	79		19	20	53	5.5	2.2
15	11.01.11	09.02.11	29	n.d.	n.d.	387	57	155		22	40	71	9.2	1.9
16	09.02.11	10.03.11	29	30 357	0.08	179	28	72		30	65	34	10.8	1.0
17	10.03.11	08.04.11	29	44 616	0.35	289	59	98		18	16	32	3.7	2.3
18	08.04.11	07.05.11	29	n.d.	n.d.	n.d.	n.d.	n.d.		6	9	20	1.9	0.4

n.d. = not determined

BGD
12, 18253–18313, 2015

Table 3. Fluxes of alkenones, the $U^{k'}_{37}$-index and the estimated SSTs for samples #1–8 of the upper trap.

CVOO-3 upper sample #	cup open	cup close	duration days	Alkenone flux ng m^{-2} d^{-1}	Alkenone unsaturation index UK'37	Alkenone SST (°C)
1	01.12.09	30.12.09	29	312.7	0.93	26.5
2	30.12.09	28.01.10	29	209.5	0.91	25.9
3	28.01.10	26.02.10	29	1852.5	0.85	24.3
4	26.02.10	27.03.10	29	700.0	0.82	23.6
5	27.03.10	25.04.10	29	464.2	0.91	26.1
6	25.04.10	24.05.10	29	227.1	0.90	25.7
7	24.05.10	22.06.10	29	1537.2	0.96	27.4
8	22.06.10	21.07.10	29	791.2	0.98	28.0
9–18				n.d.	n.d.	n.d.

n.d. = not determined

BGD
12, 18253–18313, 2015

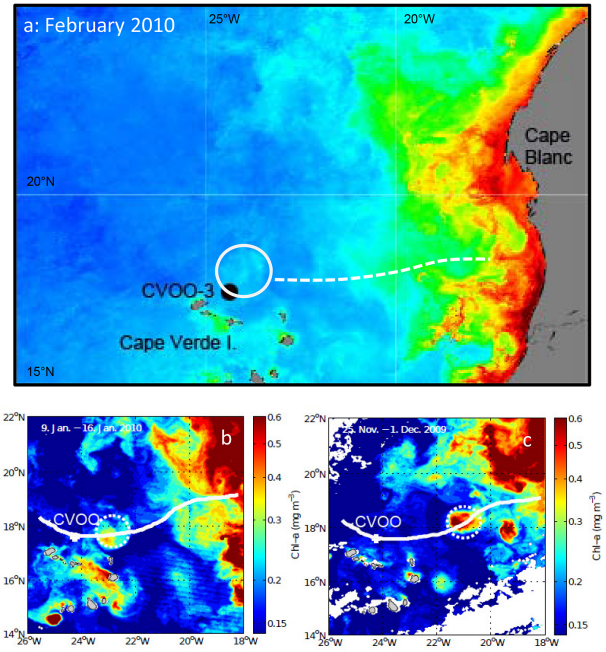

Figure 1. (a) MODIS high resolution chlorophyll picture (4 km^2, L3) with the CVOO time series site (black circle). Satellite chlorophyll within the ACME is low in February and hard to see (white circle). The pathway of the eddy from the coast in summer 2009 to the CVOO site is indicated by a white dashed line. **(b, c)** satellite chlorophyll for November/December 2009 and January 2010 (modified, Karstensen et al., 2015a). Chlorophyll decreased between November/December 2009 and January 2010, and again between January and February 2010 within the eddy.

BGD
12, 18253–18313, 2015

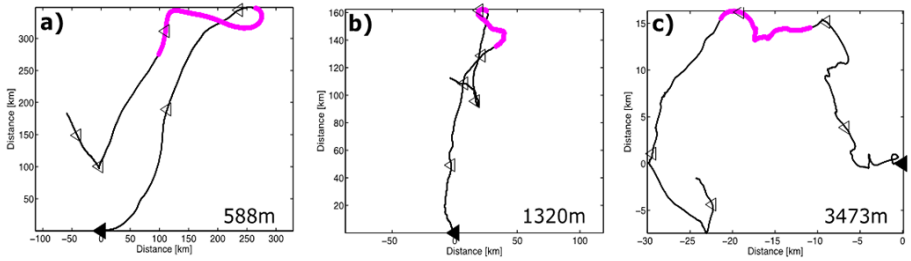

Figure 2. Progressive vector diagram (PVD) of 48 h low pass filtered current meter records at **(a)** 588 m, **(b)** 1320 m, and **(c)** 3473 m for the period from 1 December 2009 (filled triangle at 0,0) to 1 May 2010. The segment in each PVD that corresponds to the ACME passage is indicated by the magenta dots. Open triangles indicate the trap sampling intervals of 29 days. Note, for the deep trap current meter, the speed failed shortly after installment and a constant speed of 1.1 cm s^{-1} was used throughout the record.

BGD
12, 18253–18313, 2015

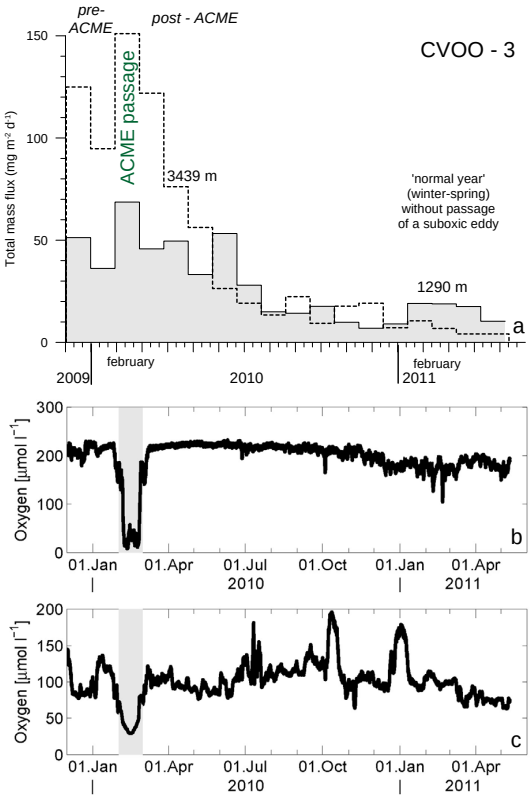

Figure 3. Total mass fluxes collected with the upper and lower sediment traps at CVOO-3 **(a)**. Oxygen time series at approx. 42 m **(b)** and 170 m **(c)** water depths (Karstensen et al., 2015a); gray bar indicates the ACME passage in February 2010. Upper and lower trap fluxes are highly correlated (r^2 = 0.7; N = 17), however, lower trap mass fluxes are roughly twice as high during winter–spring 2010 when the ACME passed the site. The common pattern can be seen in winter 2011 during the eddy-free year.

BGD
12, 18253–18313, 2015

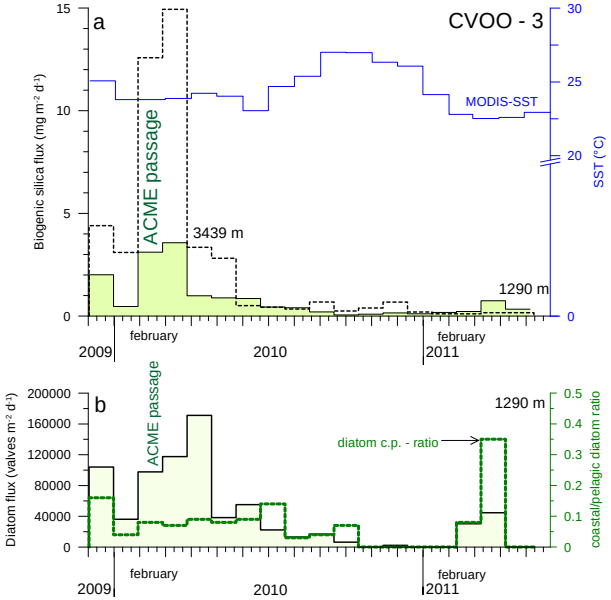

Figure 4. (a) BSi fluxes collected with the upper and lower sediment traps at CVOO-3. During ACME passage in winter 2010, BSi fluxes were more than 3 times higher in the lower trap. Fluxes in both depth levels were highly correlated (r^2 = 0.9, N = 17). Monthly mean SST from MODIS-Terra-4 km are shown for a 1 degree box to the E of the CVOO-3 site (17–18° N, 23–24° W). **(b)** Diatom fluxes (filled green bars) and the coastal : pelagic diatom ratio (green stippled line) are given for the upper traps samples.

BGD
12, 18253–18313, 2015

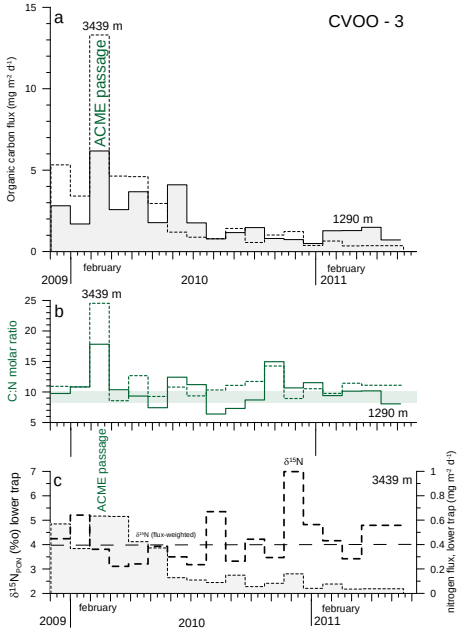

Figure 5. Organic carbon fluxes collected with the upper and lower sediment traps at CVOO-3 **(a)** and the corresponding molar C : N ratios of the organic matter **(b)**. Upper and lower trap fluxes are correlated (r^2 = 0.7; N = 17). Note the unusually high C : N ratios in February 2010 recorded in both traps. Typical molar C : N ratios (8–10) for degraded marine organic matter off NW Africa (Fischer et al., 2003, 2010) are indicated by a green stippled horizontal bar in **(b)**. **(c)** δ^{15}N values for organic matter sampled by the lower trap (stippled thick line) shown together with the total nitrogen fluxes (grey bars).. The flux-weighted mean δ^{15}N value of 3.98 is shown as well. Note the stepwise decrease in winter 2009–2010.

BGD
12, 18253–18313, 2015

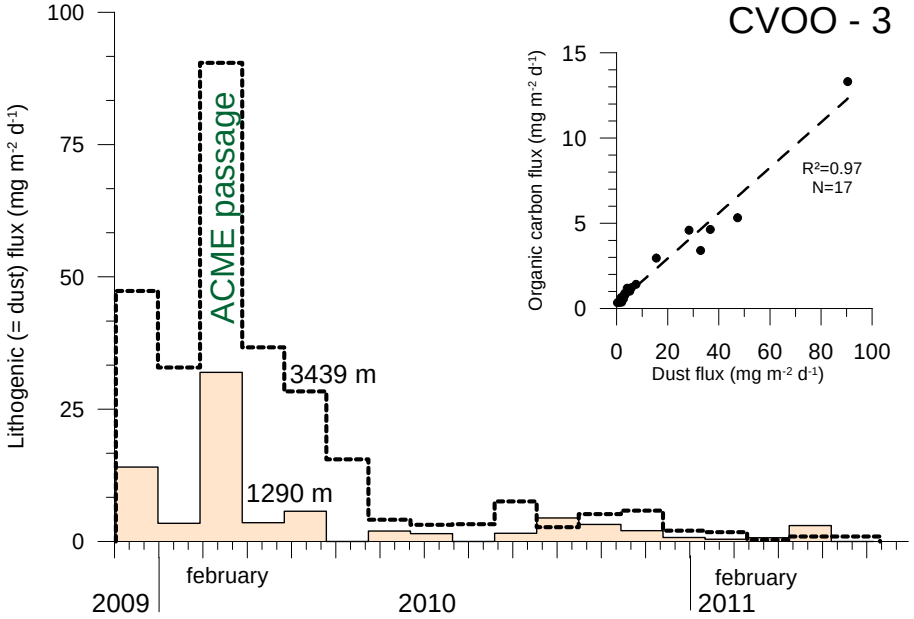

Figure 6. Lithogenic (mineral dust) fluxes collected with the upper and lower sediment traps at CVOO-3. Upper and lower trap fluxes correspond well (r^2 = 0.83; N = 17) but fluxes in the deep trap were more than twice as high compared to the upper trap during winter–spring when the ACME passed. Note the very close relationship to organic carbon (r^2 = 0.97; N = 17) shown for the deep trap samples (insert).

BGD
12, 18253–18313, 2015

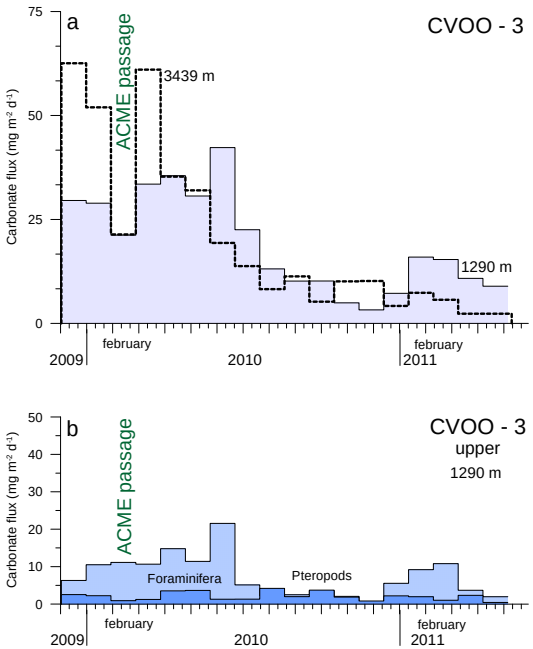

Figure 7. Carbonate fluxes collected with the upper and lower sediment trap **(a)** at CVOO-3 shown together with fluxes of planktonic foraminifera and pteropods (only upper trap data, **(b)**, Table 2). Correlation of fluxes between both depths is less significant here compared to the other components ($r^2 = 0.5$; $n = 20$). Note that total carbonate fluxes decreased during eddy passage in February 2010.

BGD
12, 18253–18313, 2015

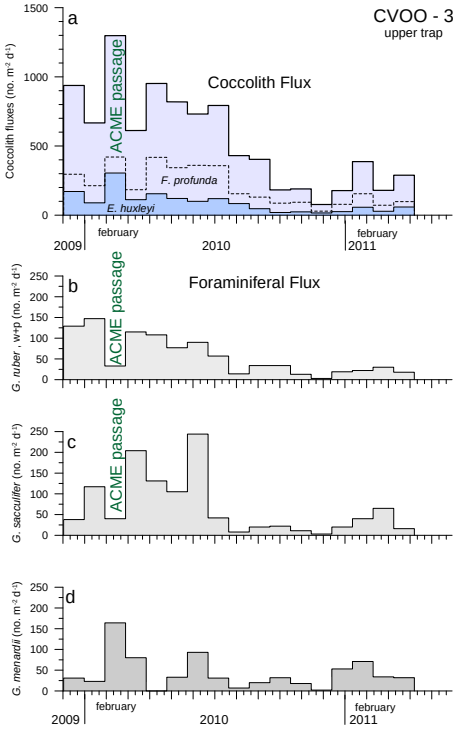

Figure 8. Upper trap fluxes of major primary and secondary carbonate producing organisms (Table 2). **(a)** Coccolithophores (total coccolith flux, flux of *E. huxleyi* and *F. profunda*). The planktonic foraminifera **(b)**: *G. ruber* (white and pink), **(c)**: *G. sacculifer* and, **(d)**: the deep dwelling *G. menardii*, the latter showing a distinct peak in flux during ACME passage in February 2010.

BGD
12, 18253–18313, 2015

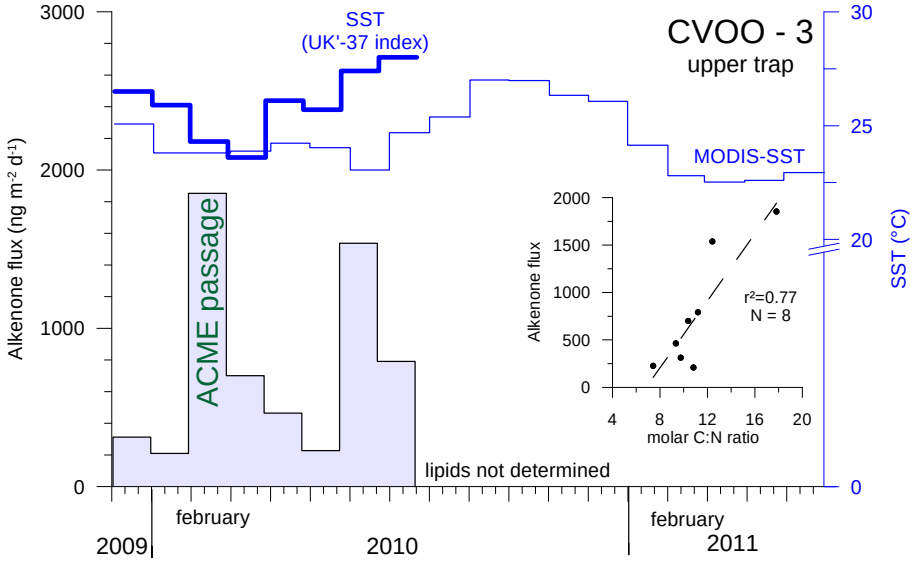

Figure 9. Alkenone fluxes together with the $U^{k'}_{37}$- derived and satellite SSTs, for the time period before and after the ACME passage. Molar C : N ratios taken from Fig. 5b which correlate to the alkenone fluxes are shown in the insert (r^2 = 0.77; N = 8). Both parameters may point to nutrient limitation at some time around the passage of the ACME.

BGD
12, 18253–18313, 2015

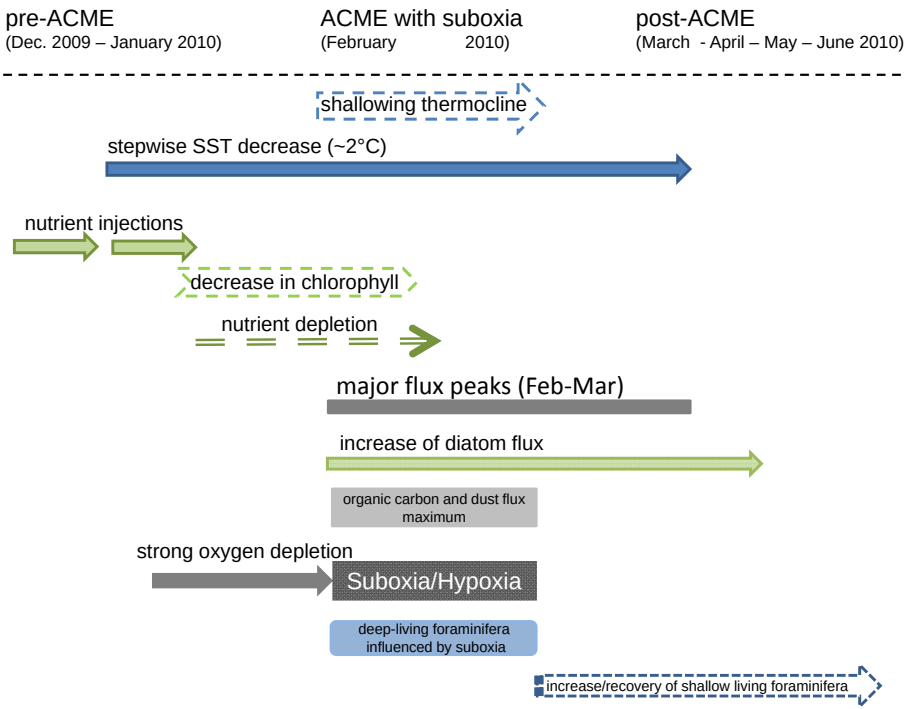

Figure 10. Schematic timeline of inferred processes within the ACME (surface waters and the suboxic/hypoxic water column below) which approached and passed the CVOO site in the beginning of 2010. Important sediment trap flux signatures are indicated. We assume a rapid transmission of the surface signature from the ACME to the bathypelagic traps of only 1–3 weeks, mainly due to high particle settling rates.

BGD
12, 18253–18313, 2015